BOILING OF LNG ON WATER: THE FOAMING PHENOMENA

by

OTTO J. SOLIS *Quintero*

B.S. Northeastern University 1976

Submitted in Partial Fulfillment

of the Requirements for the

Degree of Master in Science

at the

MASSACHUSETTS INSTITUTE OF TECHNOLOGY

December, 1977
(i.e. February, 1978)

Signature of Author: _____

Department of Chemical Engineering, Dec. 1977

Certified by: _____

Thesis Supervisor

Accepted by: _____

Chairman
Departmental Committee on Graduate Theses

ii

ABSTRACT

BOILING OF LNG ON WATER: THE FOAMING PHENOMENA

BY

Otto J. Solis

Submitted to the Department of Chemical Engineering
on December 19, 1977, in partial fulfillment of the
requirements for the degree of Master in Science.

The present study is on the foaming phenomena that
occurs when cryogenic liquids boil on a pool of water.
The cryogens studied were liquid nitrogen, methane, eth-
ane, propane, binary mixtures of the hydrocarbons and
typical LNG compositions. The cryogenic liquid composi-
tion, and the quantity of cryogen spilled per unit area
were the primary variables.

Maximum foam height occurred for the specific binary
mixtures 99% methane, 1% propane; 99% methane, 1% propane;
95% methane, 5% butane; 95% methane, 5% ethane; and LNG
compositions as 93% methane, 5% ethane, 2% propane, 85%
methane, 10% ethane, 5% propane; in all of these composi-
tions the quantity spilled was over 140 grams onto a
water surface of 129 cm^2.

Thesis Supervisor: Robert C. Reid

Title: Professor of Chemical Engineering

Dedicated to my parents,

my wife Maxula,

my son Otto Johnny.

ACKNOWLEDGEMENT

TABLE OF CONTENTS

TABLE OF CONTENTS (Continued)

LIST OF FIGURES

LIST OF FIGURES (Continued)

LIST OF TABLES

NOTATIONS

A	Area
C, C_A, etc.	Concentration
C_P	Thermal Capacity
D	Diameter
D_{AB}	(or $\mathcal{D}$) Diffusivity Coefficient
g	Acceleration of Gravity
H	Enthalpy
ΔH_v or$_f$	Latent Heat of Vaporization, Fusion or Sublimation
k	Thermal Conductivity
K	(or k) Surface Dilational Viscosity Coefficient
m	Mass or wave Number
N_{a_z}	Mass Flux
P	Pressure
ΔP	Pressure Difference
P(R)	Pressure Inside a Bubble Radius R
$P\alpha$	Pressure Outside a Bubble
P_{A_o}	Partial Pressure of Substance A

NOTATIONS (Continued)

P_A	Vapor Pressure of A
Q , $Q°$, q, q	Heat Flux
Q''	Heat Generated per Unit Volume
R	Radius of Bubble
R'	dR/dt
R	Universal Gas Constant
r	Radius
s^*	Height of Flight of a Droplet
Sc	Schmidt Number (v/D)
t	Time (sometimes θ)
T	Temperature
U	Internal Energy
u	Velocity
x	Shear stress factor, or distance
x_A, X_A	Composition in Liquid (Mole or Mass Fraction)
y_A	Composition in Vapor
z	Distance

GREEK

α	$(=k/Cp)$ thermal diffusivity
	or, relative volatility or, a constant (in Appendix A)
β	growth constant for bubbles

NOTATIONS (Continued)

γ (= $3\gamma/(2\,\Delta P R_f)$ surface tension: pressure difference ratio

δ thickness of layer (vapor film, boundary layer, i.e. discs etc.)

ε = $\rho L - \rho v/\rho L$

or, bubble node height

or, void fraction

ζ distance

η similarity parameter (= $r/2\,Dt$)

θ time

κ surface dilational viscosity coefficient

λ wavelength

μ viscosity

ν kinematic viscosity (u/ρ)

ξ distance

$\rho\ \rho\ \rho$ density

σ surface tension

τ time or period

ϕ prefactor for equation 3-5

or, dimensionless temperature

or, pressure constant

ψ (= R/R_f), a dimensionless radius. Defined differently in Appendix A.

NOTATIONS (Continued)

SUBSCRIPTS

o	Reference point
w	water
v	vapor
L	liquid
c	cryogen
T	total
f	final

Supersciipt –	average

CHAPTER 1: INTRODUCTION

1. INTRODUCTION

When pure cryogenic liquids boil, no foam is evident. In the case of LNG, foaming has been reported (LNG Foam Tests at the LNG Research Center, Massachusetts Institute of Technology, (1976), only in those cases where there was a significant fraction of heavier hydrocarbons.

Foaming most often occurs when (in a binary), the less volatile component has the higher surface tension. As bubbles form during vaporization, the liquid layer surrounding the bubble enriches in the less volatile component and the surface tension rises. By one of several possible mechanism, the net result is the pinching-off of the bubble while small. From photographs of a LNG-water interface immediately following a spill, with pure methane, the bubbles are large whereas for LNG there is a distribution of bubble sizes with many that are very small.

For rich LNG spills where bubbles are small, they rise to the surface but may be retarded from bursting since the enriched liquid layer around the bubbles is relatively nonvolatile in the cold vapor phase. Thus they accumulate on the surface and are observed as "foams".

The present study was conducted to study the "foaming phenomena" that is present when a spill of LNG occurs on a pool of water. The effect of different compositions of LNG, as well as, the quantity of LNG charged were to be emphasized.

CHAPTER 2: THEORY

2.1 GENERAL BACKGROUND

Results obtained in the literature (Je Je, 1974), indicate that the boiling rate of LNG on a water surface is extremely sensitive to composition. Even the addition of a few tenths of a percent ethane or propane to liquid methane can increase the boiling rate by 50% or more. The theory ordinarily employed to explain such rate increases involves the assumption that some ice forms very rapidly on the water surface. Nucleate boiling is initiated on the ice and then conduction (within the ice) occurs with continous water-to-ice phase transformation;when LNG is spilled on water the large temperature difference causes film boiling. Eventually the surface layer of water reaches the freezing point and ice forms, nucleate boiling is promoted and, as a consequence there is an increase in heat flux.

When LNG is spilled on water there is unquestionable some ice formed, but the photographic study (Je Je, 1974) of the liquid-liquid interface does not indicate that an ice layer is instantaneously formed, and it is not a continous layer even when formed. It was suggested that small ice crystals may be mixed in the very top layers of the water surface and remelted. There is photographic evidence to

indicate significant micro-eddy activity in the upper layers
of the water surface (Je Je, 1974).

In the literature (Drake et. al., 1975, Booth et. al.,
1974) on LNG spills it has shown that there is extensive
small bubble formation and this may be an important fact in
explaining the high LNG-water heat fluxes. The mechanism of
production of these bubbles is not known. They may have been
formed in a "nucleate boiling" type process soon after the
liquids were contacted, i. e., when the volatile liquid super-
heats on direct contact with water. Wehmeyer and Jackson
(1972) experimentally found that a wire, subject to a large
step change in temperature while immersed in a liquid pool,
produces discrete bubble first, then bubbles coalesce to form
a stable vapor film around the wire. Film boiling was not
achieved instantaneously, it is suggested that after a spill
of a cryogenic liquid on water, discrete bubbles are also
produced first when the liquids directly contact each other.
Film boiling is achieved when adjacent bubbles at the liquid-
liquid interface coalesce. Futhermore, it is suggested that
the bubbles formed in a single component cryogenic liquids
growth to relatively large sizes and coalesce readily to
initiate film boiling. But in mixtures, smaller bubbles are
formed as a result of the hydrodynamic forces on each bubble

in its early growth stage. Van Wijk, et. al., (1956) has shown that, the bubble size is a minimum at the maximum heat flux. For a pure liquid the vapor bubbles, which are at their dew point, continue to growth during their passage through the bulk of the superheated liquid. For a mixture, the dew point of the vapor bubbles is the same as the boiling point of the remainder of the mixture. Since the liquid is locally being depleted of the volatile component, the dew point of the bubbles is higher than the boiling point of the original mixture. As the bubble travels upward through a mass of superheated liquid, a point will be reached in which the dew point of the bubble equals the temperature of the bulk superheated liquid. At this location, the driving force ($T_{bulk} - T_{bubble}$) becomes zero and only diffusional interchange takes place thus keeping the size of the bubble considerable smaller than the pure boiling liquids.

Knowing that those small bubbles are present, "the foam formation" may be due to an increse heat transfer rate and a consequent increase in bubble generation. Since the bubble size is small, it will take longer time to rise through the liquid than big bubbles.

A theory different from Van Wijk to explain the small bubble formation in mixtures, was developed by Hovestreijdt, (1963).

The mixtures studied by Hovestreijdt were mostly aqueous solutions or organic substances. The higher values of q_{max} were found in so-called positive systems (in these systems the more volatile component has the lower surface tension at the same temperature). LNG is also a positive system since methane is the most volatile component, has the lower surface tension at 112°k which is 10.2 dyne/cm.

In bubbles formed in liquid mixtures the concentration of the volatile component in the vapor phase is greater than that in the liquid phase. In consequence of the formation of vapor, the amount of the volatile component in the liquid near the bubble surface is decreased and diffusion from the bulk liquid must supply this defficiency. However, if two bubbles are near to each other, the diffusion to the liquid film between both is hindered.

Thus a concentration gradient in the bubble surface is built up. The depletion of volatile component also occurs at the bases of the bubbles. If the surface tension of the more volatile component is the lower one (positive systems, LNG), the surface tension between the bubbles or at the bases of the bubbles is higher than in the other parts of the bubble surface.

The influence of this positive or negative gradient of

the surface tension on the behavior of mixtures in distillation columns was studied by Zuiderweg and Harmes (1958). With a positive mixture in a sieve plate column, the bubbles on the plate did not merge. A foam was formed which decreased the capacity and increased the tray efficiency of the column. The authors explained this stabilization of the bubbles by the fact that, in positive mixtures, due to the surface tension gradient, liquid is drawn in between bubbles approaching each other.

The transition from nucleate boiling to unstable film boiling which occurs at q_{max} is often explained by the merging of bubbles as soon as they cover the heating wall. However, the bubble density on the wall, fluctuates both in place and time, and the mean distance between bubbles at merging is larger than the actual bubble diameter. A stabilization of the bubbles against merging will decrease the mean merging distance; hence the bubble occupational density at the heating wall and the q_{max} value will be increase.

However, there are more ways through which the surface tension gradient may influence q_{max}. For instance, in positive mixtures, the bubbles are pinched off at a smaller diameters. The surface tension gradient at the bases of the bubble tend to draw liquid between the bubble and the wall.

Through this effect (which is independent of the slowing down of the bubble growth rate) an active nucleous will produce more bubbles per second and this may increase the heat exchange of the heating wall.

Apart from the influence on q_{max}, the stabilization of the bubbles in positive mixtures will result in "the foaming phenomena".

2.2 FOAMS

Introduction

The foam with which this thesis deals is composed of agglomerations of gas bubbles separated from each other by thin liquid films. Foams are dispersions of a relatively large volume of gas in a relatively small volume of liquid (Bikerman, 1953). When the volume of liquid is considerably greater than that of gas, the gas bubbles are, as a rule, shperical and their mutual interaction is weak; these systems are known as gas emulsions, and the term "gas dispersion" is also encountered. (Some scientist in English speaking countries use the German word kugelschaum or sphere foam.) The boundary between foams (sometimes denoted in Germany as polyederschaum) and gas emulsiones naturally is not quantitatively defined.

If 1 cm^3 of foam or gas emulsion contains φ cm^3 of liquid and 1 - φ cm^3 of gas, it is customary to speak of foams when φ is less than 0.1 and of gas emulsions when φ exceeds 0.9; the region in between is a "gray zone". In a true foam, the bubbles are so crowded that their shape is polyhedral; the liquid is reduced to thin films separating the polyhedrons.

Foams have a definite structure. Wherever three films come together, they form three angles of 120° each. The necessity of this arrangement is made clear in Figure (1) where A, B, and C are contiguous bubbles, and 1, 2, and 3 are the films that separate them.
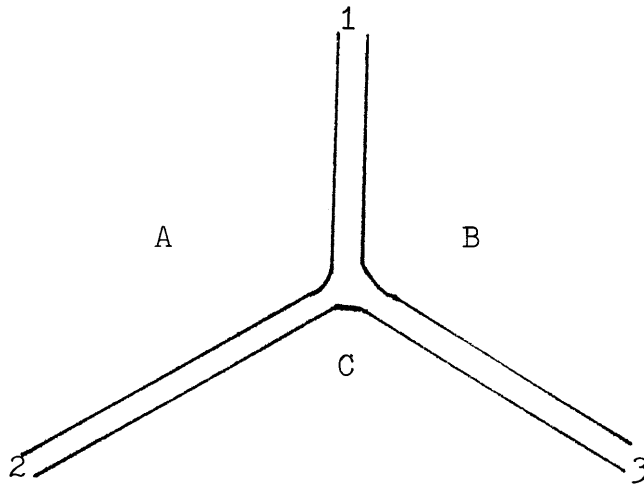
Figure 1

Three identical forces, as in the surface tension of three foam bubbles, are balanced only when the angles between them are each 120 degrees.

Each film has a contractile tendency of 2 γ per cent-
imeter; γ is the surface tension of the liquid and the fac-
tor 2 is due to the fact that each film has two liquid-gas
interfaces. Three identical forces (in this instance, 2γ
per cm) can balance each other only if the three angles bet-
ween them are identical, i.e., equal to 120° each. In a
pentagonal dodecahedron, i.e., in the three dimensional
figure formed by 12 equlateral pentagons, the internal angles
have the magnitude of 120°, and these figures almost comple-
tely fill the space. Thus, foam bubbles tend to have a
shape similar to pentagonal dodecahedrons, if their volumes
are equal.

In the vast majority of foams, different bubbles have
different volumes and, consequently, their shapes greatly
deviate from the ideal.

Formation

In common with other colloidal systems, foams can be
produced by condensation or by dispersion. In the first case,
the future gas phase is initially present as separate mole-
cules which then gather together to form bubbles. Foam on

beer is a typical example. Carbon dioxide produced by yeast first dissolves in the aqueous medium; when the pressure on the liquid is suddenly (by uncorking the bottle), the solution becomes supersaturated and the excess of solute forms a dispersed gas phase.

In the dispersion methods, the gas originally exists as a bulk phase. Small volumes of the latter are introduced into the liquid and become bubbles. The most easily controlled way of achieving this is to drive the gas through a capillary into the liquid; thus, each bubble forms singly at the tip of the capillary. In this manner, monodisperse foams (i.e., those consisting of bubbles of identical dimensions) can be obtained. Forcing the gas through a porus septum (plug) is a much quicker process but the foam produced is not monodisperse because many bubbles coalesce before breaking off the septum. Control over the properties of the foam is even poorer when the foam is produced by agitation, which may mean shaking a vessel partly filled with a liquid capable of foaming, or pouring such liquid from one vessel into another, which is the case of LNG that is poured into water, or causing turbulence with a propeller as in a commercial blender.

In all these methods, bubbles separated from each other by relatively thick liquid layers are initially produced, and

transformations of these gas emulsions into true foams usual-
ly is achieved by gravitation. The bubbles rise in the liquid
and accumulate near its top. In the process, each bubble has
to travel, at a reasonable speed, a distance of perhaps sev-
eral centimeters but then must practically stop when a film
only a few microns thick remains between it and the neighbor-
ing bubble. The reasons for this change of state are the
causes of foam stability.

Properties

Foams have some regidity even if their films are complete-
ly liquid. This is so because the structure corresponds to a
minimum surface area and, consequently, a minimum surface en-
ergy, and every deformation increases this energy - i.e., re-
quires external work. The degree of rigidity observed is
particularly remarkable when the low density of foams is
taken into consideration; an aqueous foam whose bubbles are
about 1 cm in diameter with films about 10^{-3} cm thick has a
density of about 0.003 g/cm^3.

Foams are fundamentally unstable systems. Three main
process occur in almost any foam: redistribution of bubble
sizes, film thinning, and film rupture.

The first effect is caused by the dependence of the gas pressure in a bubble on the curvature of its walls. For simplicity's sake, consider a system of two bubbles only (see Figure 2). Let the radius of curvature of the wall of the larger bubble be R_1, that of the smaller, R_2, and that of the partition (common to both) R_o. From Laplace's equation, the gas pressure in the first bubble is

$$P_a + 4\gamma/R_1$$

if P_a is the atmospheric pressure. The factor of γ is 4 because the bubble has two gas-liquid interfaces, the internal and external. In the small bubble, the gas is under pressure $P_a + 4\gamma/R_2$. To achieve mechanical equilibrium, the septum between the two bubbles must be concave toward the smaller bubble, and its radius of curvature be given by equation

$$\frac{4\gamma}{R_o} = \frac{4\gamma}{R_2} - \frac{4\gamma}{R_1}$$

or $R_o = R_1 R_2/(R_1 - R_2)$

The mechanical equilibrium would be stable if the septum were completely impermeable to the gas in the bubbles. As no
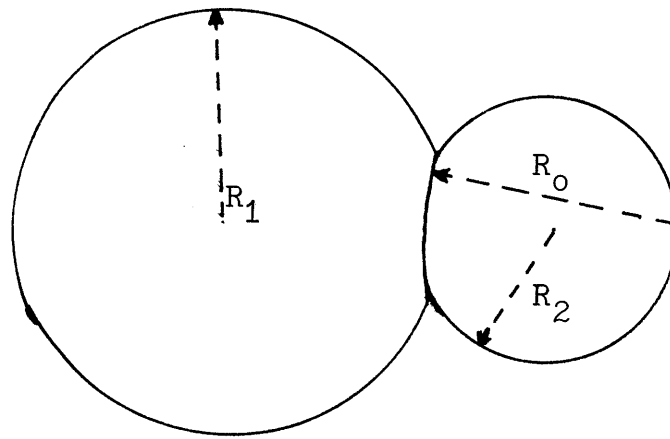
Figure 2

Gas diffuses from the smaller to the
larger bubble under the influence of
pressure differential.
(Bikerman, 1965)

such impermeability exists, gas diffuses through the wall
from the region of high into the region of low pressure.
Thus, the smaller bubble (in which the gas pressure is great-
er) gets smaller, and the bigger bubble grow. If the differ-
ence between R_1 and R_2 is initially small, gas diffusion
raises it. Thus polydispersity of foams tends to increase
on aging.

The macroscopic effect of film thinning is foam drainage.
If a vessel is filled with foam and left alone, after a time,
a layer of liquid usually appears at the botton of the vessel
and continues to grow until very little liquid remains in the
foam films (or until the film bursts). Gravitation is one of
the two reasons for film thinning. If a vertical film of thick-
ness δ and width w may be treated as a slit filled with liquid
between two plane parallel walls, then the volume of liquid
flowing downward in unit time is dV/dt = $g\rho w\delta^3/12\eta$(g is ac-
eleration due to gravity, ρ the difference between the densi-
ties of the liquid and the air around the foam, and η is the
viscosity of the liquid), Bikerman (1964). In reality, the
film gets thinner when drainage takes place - i.e., δ decreases
instead of being constant. Also the "walls" of the film usual-
ly are not solid, and their relative rigidity has a marked

effect on the rate of drainage, Epstein (1956), liquids drains
also in the veins (in which three bubble walls meet), and the
volume passing through the veins may exceed that flowing in
the walls, if δ is small.

The other reason for film thinning is suction by Plateau's
borders. The wall between A and B in Figure (1) is sensible
plane, hence liquid filling the wall is under the same pres-
sure as the gas in the two bubbles. However, the liquid-air
interface near the junction of three bubbles is concave toward
the air phase. Consequently the liquid there is under nega-
tive capillary pressure (see Equation 1), and the pressure
difference drives liquid from the inside of the wall to this
Plateau border. This pressure difference usually is much
greater than that between the gas phases in two adjacent bub-
bles. Figure 3 shows a Plateau border (pB) in a horizontal
single film, in which gravitation does not contribute to drain-
age.

Film rupture. Foam bubbles and foam films burst because
the area (and, thus, surface energy) of the resulting drop or
drops is smaller than that of the initial system. For instance,
a bubble of 1 cm radius and wall thickness of 10^{-3} cm has sur-
face area equal to approximately 25 cm^2, and if it gives rise
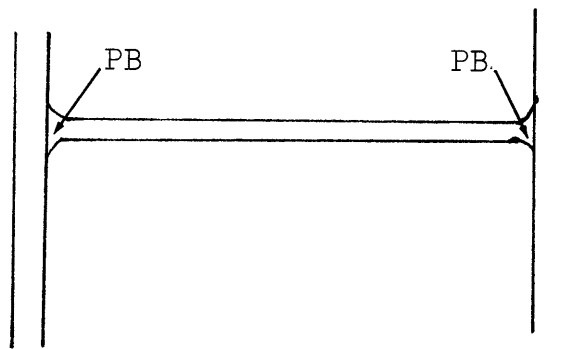
Figure   3

A Plateau border (PB) in a horizontal

single film, in which gravitation does

not contribute to drainage.

(Bikerman, 1965)

to just one droplet, the surface of the latter is about
0.2 cm^2. The energy difference is so large that, when a film
burst, the liquid in it may acquire a speed of 1000 cm/sec.
or 20 miles/hr.

Nevertheless, foams can persist for measurable time.
Single films, as illustrated in Figure 3, are produced and
their life time τ can be measured. Or the lifetime τ of a
bubble, which rises to the surface of the liquid, before burst-
ing can be determined. This τ is smaller the greater the film
or the bubble, and usually greatly depends on the humidity of
the atmosphere, on convection currents, etc. It may be con-
cluded, therefore, that bursting is caused not by processes
inherent in the film but by external agents.

2.3   BUBBLE GROWTH THEORIES

Existing theories deal primarily with the spherical symmetric growth of a single bubble in an infinite body of a liquid at rest. It is generally recognized that a bubble grows in three stages:

1. The inception or formation of an embryo (a process thermodynamically defined).

2. An early growth of the embryo. (This is a dynamic process controlled by the pressure forces, surface tension and inertia of the liquid.)

3. A late or asymptotic growth stage which is diffusion controlled. The supply of the enthalpy of vaporization by conduction and convection from the liquid bulk to the expanding bubble walls limits the bubble growth rates. Diffusion of material is also important in liquid mixtures. Only the latter two stages are of interest in the present work.

Survey of the Literature

Equations describing the growth of a single spherical bubble has been formulated by Plesset and Zwick (1954), Scriven (1959) and Skinner (1963) among others. Solutions to the

equations have, however, been sought mostly for the asymptotic grow stage. The available solutions agree very well with the experimental data of Dergarabedian (1953, 1960) and Van Strahalen (1967, 1968).

The pertinent equations and boundary conditions describing the growth of a single bubble are presented in the complete forms in Table 1. Equations 3 and 5 are employed only when liquid mixtures are involved.

The complete set of equations has not been solved, but solutions exist when simplifying assumptions are made, especially in the asymptotic growth regime. Most solutions (e.g. Plesset and Zwick, 1954) assume the existence of a thermal or concentration boundary layer around a growing bubble, negligible viscous effects, zero bubble translational velocity, no temperature or concentration gradients within the bubble, negligible compressibility effects due to rapid growth, and thermal equilibrium between the bubble contents and surrounding wall. Moreover, a bubble is assumed to growth as a result of and controlled by heat and /or mass transfer from the surrounding superheat liquid, across the growing boundary layer.

TABLE 2.1

BUBBLE GROWTH EQUATIONS

A.   Equation of motion (Scriven, 1959, 1962)

$$RR'' + \left(2 - \frac{\varepsilon}{2}\right) R'^2 + 4\nu\frac{R'}{R} = \frac{P(R) - P_\alpha}{\varepsilon \rho_L} \qquad (1)$$

where $P(R) = P_b - \frac{2}{R}\left(\sigma + 2k\frac{R'}{R}\right)$ (1.a)

B.   Energy equation (no sources)

$$\frac{\partial T}{\partial t} = \alpha\left(\frac{\partial^2 T}{\partial r^2} + \frac{2}{r}\frac{\partial T}{\partial r}\right) - \frac{\varepsilon R' R^2}{r^2}\frac{\partial T}{\partial r} \qquad (2)$$

C.   Material balance on the more volatile component of a binary mixture (no chemical reaction)

$$\frac{\partial X_A}{\partial t} = D_{AB}\left(\frac{\partial^2 X_A}{\partial r^2} + \frac{2}{r}\frac{\partial X_A}{\partial r}\right) - \frac{\varepsilon R' R^2}{r^2}\frac{\partial X_A}{\partial r} \qquad (3)$$

Equations (1) to (3) must satisfy the following boundary conditions :

$$4\pi R^2 \, k\frac{\partial T(R,t)}{\partial r}\bigg|_{r=R} = \sum_i \Delta H_{v_i} \frac{dm_i}{dt} + \Delta H_{mixing} \frac{dm}{dt}$$

$$+ \frac{\partial(mC_pT)}{\partial t} \qquad (4)$$

where $m = 4/3 \, \pi R^3 \, \rho_v$

and $m_i = Y_i m$ (Y_i is mass fraction of compo-

nent i inside the bubble)

$$-4\pi R^2 \rho_L \, D\frac{\partial X_A}{\partial r}\bigg|_{r=R} = X_A \frac{dm_B}{dt} - X_B \frac{dm_A}{dt} \qquad (5)$$

($X_{A \text{ or } B}$ is the mass fraction of component A or B in
the liquid)

Other conditions include the initial bubble size and the
bulk fluid temperatures and concentrations.

Single-Component Liquids

Bošnjakovic (1930) derived the equation for growth of a
bubble as:

$$k \frac{\partial T(R, t)}{\partial r} = \rho_V \Delta H_V R'$$

(6)

where the temperature profile is assumed to be the same as ob-
tained in transient heat conduction into a semi-infinite body,
with a constant temperature (different from the bulk) suddenly
imposed upon the plane boundary. (This eliminates the neces-
sity of solving Equation 2.) Equation 6 means simply that the
heat conducted from the bulk liquid to the bubble boundary
(which is at the liquid's boiling point) is entirely applied
for vaporization and, therefore, bubble growth.

For the semi-infinite body (Carslaw and Jaeger, 1959):

$$\left. \frac{\partial T}{\partial z} \right|_{z=0} = \frac{\Delta T}{\sqrt{\pi \alpha t}}$$

(7)

Hence, if the bubble curvature is neglected,

$$\frac{\partial T(R, t)}{\partial z} = \frac{\Delta T}{\sqrt{\pi \alpha t}}$$

(8)

and the bubble radius is given by

$$R(t) = \left[\frac{2k\Delta T}{\Delta H_v \rho_v (\pi\alpha)1/2} \right] t^{1/2} \qquad (9)$$

i.e., the bubble radius R(t), ($=kt^{1/2}$), is proportional to $t^{1/2}$

Plesset and Zwick (1952, 1954) presented a more comprehensive, but still approximate, solution based on a perturbation technique. Lagrangian transformations of the equations of motion and thermal diffusion were carried out. The zeroth-order solution of the unsteady state temperature profiles (equation (2), after transformation) was employed to estimate the term $\frac{P(R) - P_\alpha}{\varepsilon \rho_L}$ in Equation (1) (equilibrium was always assumed between the bubble walls and the vapor within the bubble, and the surface dilational viscosity* term was not considered). The leading term of the asymptotic solution of Equation (1) gave

-----
*The significance of this term was pointed out in subsequent studies by Scriven (1960, 1962).

$$R(t) \simeq \sqrt{3} \left[\frac{2k\Delta T}{\Delta H_v \rho_v (\pi\alpha)^{\frac{1}{2}}} \right] t^{\frac{1}{2}} \tag{10}$$

This equation is different from Equation (9) only by the constant $\sqrt{3}$.

Forster and Zuber (1954) derived another approximate solution by considering the walls of the expanding bubble to constitute a spherical heat sink. The bubble wall temperatures (always equal to those of the vapors) were obtained as time-variables by an integration of the Green's function. The derivation of the bubble wall temperature-time relation implicitly involved the concept of discontinuous bubble growth. The final solution for the late or asymptotic growth stage was given by :

$$R(t) \simeq \frac{\pi}{2} \left[\frac{2k\Delta T}{\Delta H_v \rho_v (\pi\alpha)^{\frac{1}{2}}} \right] t^{\frac{1}{2}} \tag{11}$$

The early growth of the bubble from a critical embryo radius Ro, requires that a thermal or kinetic impulse be present. If a constant local heat flux, Q' is supplied for the short early growth duration, and the hydrodynamic forces on the bubble growth are neglected,

the early growth rate is given by :

$$R(t) \simeq \frac{1}{\sqrt{2}} \left[\frac{\sigma Q'}{\rho_L^2 C_{P_L} R_o \Delta T} \right]^{1/2} t^{3/2} \qquad (12)$$

or

$$\simeq \frac{1}{2} \left[\frac{\rho_V \Delta H_V Q'}{\rho_L^2 C_P T_{bpt}} \right]^{1/2} t^{3/2} \qquad (13)$$

R_o is the initial stable-equilibrium bubble radius, and the Clausius-Clapeyron equation has been applied to obtain Equation (13) from (12). It is seen from Equation (13) that the early growth rate estimated from Forster and Zuber's analysis is independent of the superheat in the liquid.

Scriven (1959) presented exact solutions for the asymptotic growth stage based on a similarity analysis of the boundary value problem. His final expression, for a moderate superheating of the liquid ($\Delta T \geq 0.25°C$), is identical with the zero-order solution of Plesset and Zwick (1954), Equation (10)

It should be noted from the foregoing that the asymptotic solutions to the equations in Table 1, as derived by Plesset and Zwick (1954), Forster and Zuber (1954) and Scriven (1959), differ only by a multiplier ($\sqrt{3}$ or $\pi/2$) from Equation (9) more simply derived by Bošnjakovic (1930).

Bubble Growth in Liquid Mixtures

The rate of growth of a single bubble in a pure liquid
(uniformly superheated) is controlled, in the asymptotic
stage, by heat fluxes towards the bubble walls. In mixtures,
both mass fluxes of the mixture components and heat fluxes
are important. The more volatile component is rapidly and
continuously depleted from the boundary as the bubble expands,
and a concentration profile develops within the liquid adjacent
to the wall.

Van Wijk, Vos and Van Strahlen (1956) proposed that the
early growth of a bubble occurs discontinuously by flash vapor-
ization in the superheated liquid mixture. At the end of this
growth stage, both thermal and concentration equilibrium exist
between the bubble wall and vapor within. The final bubble
wall temperature, T_b, (the same as the dew temperature of the
vapor), is less than the temperature of the superheated bulk,
T_α, but higher than the saturation boiling point of the mix-
ture, $T_{b_{mix}}$. The difference, $T_\alpha - T_b$, is the superheat avail-
able for further bubble growth in the asymptotic stage.
Van Wijk et al. pointed out that, for a binary mixture,
$T_\alpha - T_b$ attains a minumum (or $T_b - T_{b_{Pmix}}$, maximum) value at
a low concentration of the more volatile component, Hence,
they suggest that the subsequent bubble growth rates will be

a minimum at this concentration. The corollary is that, after a specified asymptotic bubble growth period, the bubbles with the highest T_b at the start of the late growth stage will also have the smallest diameters. The radii of the bubbles formed at the end of flash vaporization was implicity assumed constant, or even zero. Scriven (1959) was first to quantitatively describe bubble growth in mixtures. Considering the asymptotic growth state to be controlled by the combination of heat and mass transfer, he showed that an exact similarity solution can be found for a binary mixture with constant initial temperature and composition. He presented a solution valid for moderate superheats

as: $\qquad R(t) \;=\; 2\beta(\alpha t)^{1/2}$ $\hspace{3cm}$ (14)

where
$$\beta = \left(\frac{3}{\pi}\right)^{1/2} \left\{ \cfrac{\Delta T}{\dfrac{\rho_v}{\rho_L}\left(\dfrac{\Delta H_v}{C_{p_L}} - \left[(m_A \rho_L - C_{A\alpha})\left(\dfrac{\alpha}{D_{AB}}\right)^{1/2}\right]\left|\dfrac{\partial C_A}{\partial T}\right|_p\right)} \right\}$$

$$\left.\frac{\partial C_A}{\partial T}\right|_p \simeq \frac{-C_{A\alpha}\Delta H_{v_A}\left[M_B C_{A\alpha} + (\rho_L - C_{A\alpha})M_A\right]}{\rho_L R T_{sat}^{\,2}} \left[\frac{1 + \alpha\ell}{1 - \alpha}\right]$$

$$\alpha = \gamma_B p_B / \gamma_A p_A \qquad \text{(relative volatility)}$$

and $\ell = \left[\Delta H_{v_B}(\rho_L - C_{A\alpha})\right] / \Delta H_{v_A} C_{A\alpha}$

(γ_A or $_B$ is activity coefficient)

For water-ethylene glycol mixtures, he showed that
attains a minimum with about 5% by weight of water present
in the bulk liquid, i.e. $C_{A\alpha}$= 0.05. At this composition,
water is rapidly depleted from the bubble boundary, while at
the same time, the wall temperature has been sufficiently de-
pressed below the bulk liquid's and vaporization of the glycol
occurs relatively more slowly. Again, the initial bubble
diameter was taken to be zero.

Bubble growth rates in mixtures are further slowed down
in the asymptotic stage if the bubbles are crowded, and inter-
bubble pacing is of the order of the concentration boundary
layer thickness. The experiments of Luborsky (1957) on the
growth of a large population of spherical iron crystallites
in mercury (a liquid-solid system) show that the spheres grew
at rates given by:

$$\frac{dR}{dt} \approx (1 - p^{1/3})$$

(p is volume fraction
of iron crystallites)

and
$$R^{4.4} \approx t$$

These represent considerably slower growth rates than predict-
ed for single bubbles (Scriven, 1959). It is not an unexpect-
ed growth rate since the concentration driving force decreases
as material was depleted from the interstices between adjacent
crystallites. The exact relation obtained may only have been

predicted, however, if the lattice distribution of the growing spherical bodies is provided.

Van Strahlen (1968, pt II) showed a similar effect of the depletion of a mixture component on the growth rates of swarms of bubbles.

2.3.1 SURFACE TENSION EFFECTS ON BUBBLE GROTH

The theories presented in the previous section dealt with the asymptotic stage of the growth of single bubbles within slightly superheated liquids. The diameters of the bubbles at the start of this stage of growth were assumed small, sometimes negligible. However, the photographs presented by Van Strahlen (1968) may be interpreted to suggest that this is not the case. Bubbles which grew on a heat horizontal wire ($T_{wire} \sim T_L + 20°C$) immersed in slightly superheated boiling liquids, i.e., liquids 0.2 to 1°C above the boiling point, attained large diameters in very short times after inception. About 50 to 80% of the ultimate bubble diameters (at 10 ms after formation) appear to have been realized within the first 0.2 ms. This is a period which included the early growth stage during which forces on the bubbles primarily control the growth rates. Furthermore, bubble diameters, after this initial rapid growth, were smaller in positive* liquid mixtures than in pure liquids, e.g., the Ketone-water used by Van Strahlen (1968, pt II). The small bubble sizes have generally been attributted

-----

*In these systems the more volatile component has the lower surface tension at the same temperature.

to heat/mass transfer rate limitations at the bubble walls.
The assumption of diffusion control is the basis for the solu-
tions presented earlier. The analysis of Plesset and Zwick
(1954) included an examination of the regimes at which the
dynamics or heat transfer effects are predominant. In the
paper, they treated variations in liquid surface tension as
negligible.

In this section, a simple tentative analysis is present-
ed on the effects of surface tension variations on the growth
rates of a single bubble. Any effects should be primarily
exhibited in the early growth periods of dynamic control in
the real situation. An increase in surface tension forces
at a growing bubble boundary would have the effect of slowing
down the growth rate, in addition to the heat/mass transfer
rate limiting effects. Time-dependent surface tension may
be realized for a bubble growing in a positive mixture, such
as LNG.

Here, only the equation of motion and the appropriate
forces are considered. The bubble is assumed to be spherical
and located in an inviscid fluid. Compressibility effects
are neglected. Neither the diffusion of material or energy
is allowed to limit the growth of the bubble.

The growth equation is:

$$RR'' + \frac{3}{2} R'^2 = \frac{P(R) - P\alpha}{\rho_L} \qquad (15)$$

where

$$P(R) - P_\alpha = P_b - P_\alpha - \frac{2\sigma(X_A)}{R}$$

i.e., the term $2K\frac{R'}{R}$ in Equation (1.a) has been neglected, and σ is a function of composition.

The problem may be further simplified if the bubble growth is assumed to be isothermal and the other mixture components nonvolatile. These assumptions appear to be approximate for cryogenic hydrocarbon mixtures. As shown in Figure (4), the saturation temperatures of LNG slowly increases with ethane fraction until the mixture contains less than 40% methane. Moreover, at T = -160°C, the vapor pressure of ethane, the next most volatile alkane, is only 1 mm Hg.

On substituting for P (R) - P_α , Equation (15) becomes
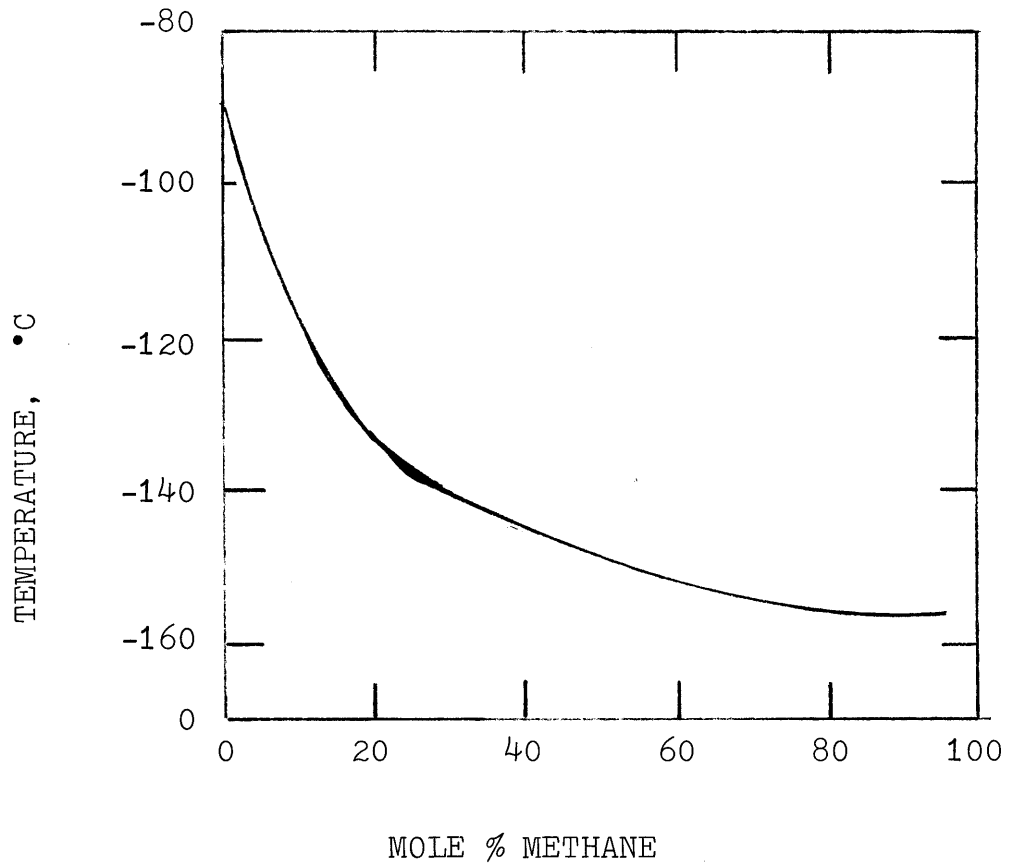
Fig.   4

Saturation Temperature of LNG (primarily
methane and ethane) As a Function of
Composition.
(derived from the data of Enger and
Hartman, 1972)

$$RR'' + \frac{3}{2} R'^2 + \frac{2\sigma(X_A)}{\rho_L R} = \frac{\Delta P}{\rho} \qquad (16)$$

Two further assumptions are made to make Equation (16) tractable. The first is that ΔP acting counter to bubble growth is a constant*. The second is that the bubble wall instantaneously attains and maintains a constant surface concentration (not necessarily in equilibrium with the vapor). This is logical if one remembers that the bubble growth rate is much faster than the rate at which the vaporized component is replenished by convective and diffusion processes. Hence, the lining of the bubble wall will contain essentially the nonvolatiles. The flux of material, determined by the concentration gradient at the wall is, however, sufficiently high that the transport process is non-limiting. The assumption of a constant X_A is made to keep $\sigma(X_A)$ constant. Note: $\sigma(X_A)$ depends on the mixture constituents, the ratios of these constituents, and temperature.)

For $P(R) - P_\alpha$ equals zero, a trivial solution is

-----
*Both this pressure difference and surface tension forces oppose the bubble growth which is initiated by an impulse. The impulse may be kinetic (inertia of the liquid) or thermal (Gibson, 1972). The bubble pressure is assumed constant and slightly less than the external value.

R = a constant

i.e., R' = R" = 0, and the bubble exists in stable equilibrium.
In general,

$$R(t) = (K_1 \ t + K_2)^{2/5}$$

where K_1 and K_2 are constant.

For $\Delta P = 0$, i.e., only surface tension retards the bubble
growth, Equation (16) can be integrated to give

$$R'^2 = \frac{2\sigma}{\rho_L} \left[\frac{R_f^2 - R^2}{R^3} \right] \tag{17}$$

where $R = R_f$ when $R' = 0$

For $\sigma = 0$, Equation (16) becomes the Rayleigh equation,
and

$$R'^2 = -\frac{2}{3} \frac{\Delta P}{\rho_L} \left[\frac{R_f^3 - R^3}{R^3} \right] \tag{18}$$

The general first level integration of Equation (16) is
approximately given by:

$$R'^2 = \frac{2\sigma}{\rho_L} \left[\frac{R_f^2 - R^2}{R^3} \right] - \frac{2}{3} \frac{\Delta P}{\rho_L} \left[\frac{R_f^3 - R^3}{R^3} \right] \tag{19}$$

where $R = R_f$ when $R' = 0$ at $t = \tau_f$. The implication of this

condition is that the bubble growth stops at τ_f, a time which marks the beginning of the asimptotic stage. This is not true. But a comparison of the bubble diameters during the early and asymptotic growth stages (Van Strahlen, 1968; Fig. 9, 12, pt II) shows that the rates of growth differ considerably. Hence, R' = 0 at t = τ_f is a fair approximation for the boundary condition.

Equation (19) can be transformed with $\psi = R/R_f$ into

$$\psi'^2 = \gamma^+ \left[\frac{1 - \psi^2}{\psi^3} \right] + \Phi \left[\frac{1 - \psi^3}{\psi^3} \right] \tag{20}$$

where

$$\gamma^+ = \frac{2\sigma}{\rho_L R_f^3} \quad \text{and} \quad \Phi = -\frac{2}{3} \frac{\Delta P}{\rho_L R_f^2}$$

Equation (20) can be re-written as

$$\psi'^2 = \frac{\Phi}{\psi^3} \left[(1-\psi^2)\gamma + (1-\psi^3) \right] \tag{21}$$

where

$$\gamma = \frac{\gamma^+}{\Phi} = -\frac{3\sigma}{\Delta P R_f}$$

This equation satisfies the conditions

$$\psi(o) = 0 \quad , \quad \psi(\tau_f) = 1 \quad \text{and} \quad \psi'(\tau f) = 0$$

Hence,

$$-\Phi^{1/2} t = \int_o^\psi \frac{\psi^{3/2} \, d\psi}{\left[(1-\psi^2)\gamma + (1-\psi^3) \right]^{1/2}} \tag{22}$$

The integral in Equation (22) has been evaluated for 3 values of γ. Calculations show that, for a given ΔP or $_\Phi{}^{\frac{1}{2}}$, the growth period (up to 0.99 max.) or $\gamma = 5$ is less than half that for $\gamma = 0$ (i.e., $\sigma = 0$, or R_f and ΔP infinitessimal).

It may therefore be concluded that if bubbles grow faster in pure liquids than in mixtures due to the smaller net growth retarding force and, as just shown above, the early growth duration decreases as the surface tension increases, much larger bubbles could be formed in pure liquids than in mixtures. Unfortunately, the values of ΔP for boiling in saturated liquid mixtures are not available in the literature, so that the relative ratios of R_f (pure liquids: mixtures) cannot be compared.

A more complete analysis of the growth of a bubble requires that a solution be found for the coupled dynamic and diffusive processes. Experimental data on transient concentration and temperature profiles, and surface tension at the bubble boundary are needed.

2.3.2 CONCENTRATION PROFILES AROUND A GROWING BUBBLE

The concentration profile at the wall of a bubble growing under isothermal conditions is described by Equation (3) subject to the boundary conditions that

$$X_A = X_{AS} \quad \text{a constant at the bubble wall}$$

and $\quad X_A = X_{A\alpha} \quad$ far from the bubble

This problem is similar to that of solid-liquid phase changes analyzed by Chambré (1956). If the growth of a shperical bubble, within a constant temperature environment is described by

$$R(t) = 2\beta\sqrt{Dt} \tag{23}$$

i.e., an asymptotic stage growth rate, a similarity concentration profile within the surrounding fluid, for Schmidt number (ν/D) equal unity, is given by:

$$\frac{x - x_{A\alpha}}{x_{AS} - x_{A\alpha}} \simeq \frac{4}{\sqrt{\pi}} \frac{\left(\frac{\rho_L}{\rho_V}\right) \beta^3 e^{\beta^2} \Xi_n}{\left[\frac{2}{\sqrt{\pi}} + \left(\frac{\rho_L}{\rho_V}\right)\beta^3 e^{\beta^2}\Xi_\beta\right]\Lambda} \tag{24}$$

where $\quad \Xi_n = \frac{2}{\sqrt{\pi}} \frac{e^{-n^2}}{n} - 2\left[1 - \operatorname{erf}(n)\right]$

Ξ_β is the same with β substituted for

$$\Lambda \simeq \frac{2}{\sqrt{\pi}} + \left(\frac{\rho_L}{\rho_v}\right)\beta^3 e^{\beta^2} \left\{ \frac{2}{\sqrt{\pi}}\left[\frac{e^{-\beta^2}}{\beta} - \frac{e^{-\eta^2}}{\eta}\right] - 2\left[\mathrm{erf}(\eta)\right.\right.$$

$$\left.\left. - \mathrm{erf}\,(\beta)\right]\right\}$$

$$\eta = \frac{r}{2\sqrt{Dt}}$$

and r is distance within the liquid measured from the bubble centroid.

The appropriate expression is considerably more complex if Schmidt number (Sc = v/D) is not unity. This is the case for diffusion within liquids. The concentration profile is, in such cases, evaluated from

$$\frac{x - x_{A\alpha}}{x_{AS} - x_{A\alpha}} \simeq 2(Sc)\ \frac{\rho_L}{\rho_v}\ \left(\frac{2}{\sqrt{\pi}}\right)^{2(Sc)}\beta^3 e^{(Sc)\beta^2}\int_\eta^\alpha \Omega^{(Sc)}$$

$$\frac{dt}{t^2} \tag{25}$$

where

$$\Omega \simeq e^{-t^2}\left[\frac{2}{\sqrt{\pi}} + \frac{\rho_L}{\rho_v}\beta^3 e^{\beta^2}\frac{2}{\sqrt{\pi}}\int_\beta^\eta \frac{e^{-S^2}}{S^2}dS\right]^{-2}$$

It can be shown from these expressions that the thickness of the concentration boundary layer is given approximately by:

$$\delta \simeq (4 - \frac{\rho_V}{\rho_L}) \sqrt{Dt} \qquad\qquad (26)$$

Hence δ may be extremely small if the growth times are very short or β large. For the early growth rate not described by $R(t) = 2\beta\sqrt{Dt}$, attempts to arrive at solutions for the concentration profiles by quadrature may not yield useful results. With $R(t)$ known, the concentration profiles could, however, be determined by involved numerical techniques.

For estimation purposes, one may assume that Equation (26) is obeyed with

$$\left(\frac{\rho_V}{\rho_L}\right)\beta \ll 2$$

Therefore, one obtains

$$\delta \simeq 4\sqrt{Dt} \qquad\qquad (D \sim 10^{-5} \; cm^2/s \; \text{in liquids})$$

If the time for growth of each bubble is chosen (arbitrarily) to be 1 ms, one obtains that the concentration boundary layer thickness is given by

$$\delta \sim 4 um$$

For bubbles formed on external surfaces, a concentration gradient may exist along the bubble wall due to the different

life times of bubble surface segments. This gradient may
cause convective flows in the neighborhood of the bubble.*
The net effect is that bubbles separated by more than 4 um
may be prevented from coalescing by the liquid flow in the
interstices. This is an extremely small separation distance.

For bubbles formed at a cryogenic liquid mixture-water
interface, a dense population of bubbles may, therefore, be
required before film boiling is initiated. The generation
of these bubbles most probably causes a local enrichment of
the less volatile mixture component.

-----
*Such concentration induced flows were studied by Blair and
Quinn (1969), Saville (1973) among other. The induced flows
are commonly known as the "Marangoni" effect.

2.4   MECHANISM OF ICE FORMATION AT A WATER SURFACE

The saturation boiling temperatures of the volatile liquids layered on water in the present investigation are much lower than 0°C. Any ice formation would be expected, therefore, to originate at the water surface.

Most of the available literature on ice nucleation and growth has been on homogeneous and heterogeneous nucleation of ice in the bulk of liquids, especially in form of drops. These studies have succeeded in determining the degree of cooling below 0°C that water can be exposed to before spontaneous ice formation occurs. Typical of the results was the data of Biggs (1953) and Langham and Mason (1958) reproduced in Figure (5) for homogeneous and heterogeneous nucleation in the bulk of water.

The mechanism of ice formation and growth at water surfaces are essentially of two types, i.e., those that lead to the formation of frazil ice and those that favor hydrates.

a.   Frazil Ice

Frazil ice consist of thin, free floating rounded discs of transparent ice, which on coalescing, followed by regela-
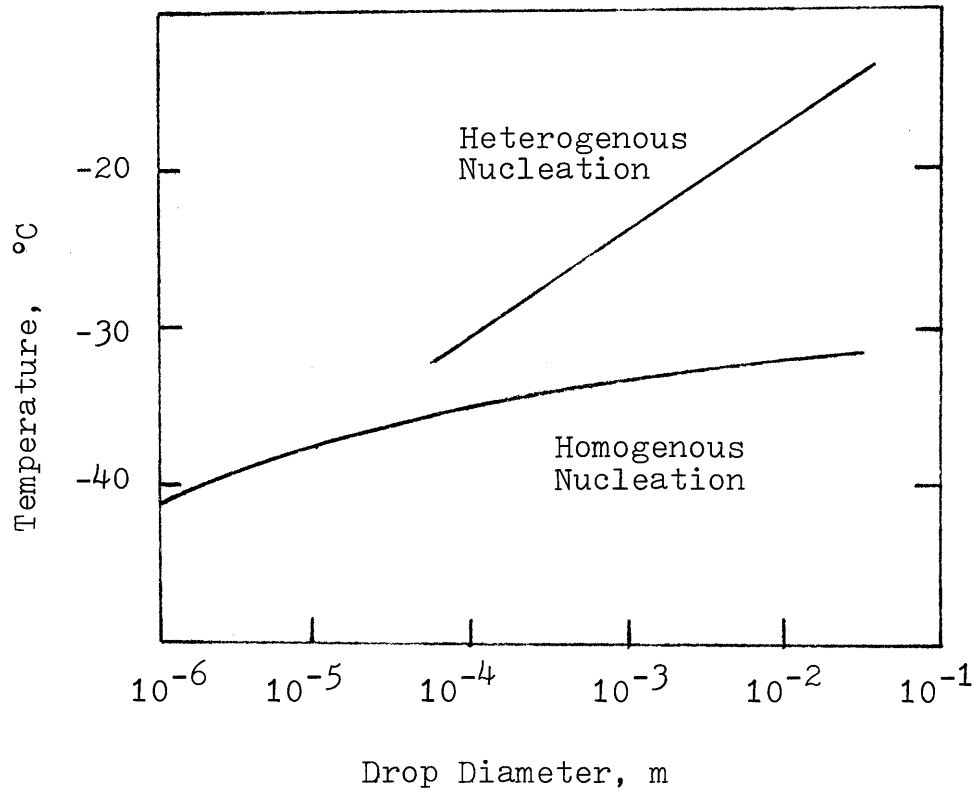
Fig. _5_

Homogenous Nucleation of Ice in Water
(mason, 1958)

tion, can form large ice masses in cold flowing streams.

The formation of frazil ice on water seldom requires that the water be cooled below -1°C. This was noted by Schaefer (1950) and Arakawa (1954, 1955). This subcooling is much less than the 20 to 40°C below zero required for nucleation in bulk water with cold flowing water. Schaefer noted that rarely more than 0.01°C supercooling was required for frazil ice to form and grow on the surface, as long as the ambient air was at temperatures considerably below 0°C ($<$ -10°C). The surface of the water must also be seeded with particles of ice. Other solid particles, such as dust, might also be suitable seeds. Futhermore, he reported that the thickness of the discs were between 25 and 100 mm for crystals to 5 mm diameter.

Arakawa (1954), working with stationary cooled shallow dishes of water, observed the same discs on water whose bulk temperature was between 0.1 and 1°C. Moreover, the discs lost their circular profile at diameters between 2 and 3 mm to become six-sided stellar dendritic crystals.

The mechanism of frazil ice formation might be described as follows. Water at temperatures higher than -1°C will not nucleate ice, even in the presence of solids in suspension in

the water, as suggested in Figure (5). The free surface of
water exposed to much colder ambient air, however, becomes
cooled to low temperatures within a small boundary layer.
The density inversion of water makes the attained tempera-
ture gradient stable, modified but not destroyed by convec-
tion currents in the underlying liquid.

The introduction of a seed within the boundary layer
zone provides low energy sites where the growth process can
start (heterogeneous nucleation). Ice particles, with the
proper surface energies and growth planes will, therefore,
be the most effective seeds. The thickness of the ice discs
will be determined by the thickness of the cooled boundary
layer and lateral growth of ice along the surface will be
fastest than the growth in the zone of maximum supercool.

b. Hydrates

Hydrates are members of the class of clathrates, i.e.,
inclusion compounds in which a molecule of one substance is
caged in a correctly-sized cavity created by rigid arrange-
ments of molecules of a substrate, with no strong chemical
bonding established between the substances.

Low molecular weight hydrocarbons and inert gases are

known to form hydrates with water under appropiate temperatures and pressures. These are solids which resemble ice or wet snow in appearance. They float on water and show densities of 0.88 to 0.9 g/cm^3. Detailed studies on hydrates established the conditions under which they form (Hammerschmidt, 1934, Deaton and Frost, 1946, a and b; Katz et al., 1959). The lattice structure have also been established (Saito el al., 1964, 1965).

The principal conditions of formation are that liquid water must be present in contact with the gas of interest, (or at least, the gas must be saturated with water vapor), at appropiate pressures and temperatures. The hydrate forming conditions are presented in Figure (6) for paraffin dydrocarbons. Katz (1959) also presented data to show that mixtures of the hydrocarbon gases form hydrates on water conditions intermediate to that required by the pure components.

Figure (6) shows the pressure at which hydrates are formed decreases with decreasing temperatures. No data are available below 0°C, but it can be hypothesized that, at sufficiently low temperatures, hydrates would form at 1 atm. with methane etc. in the presence of water.

TEMPERATURE, °F
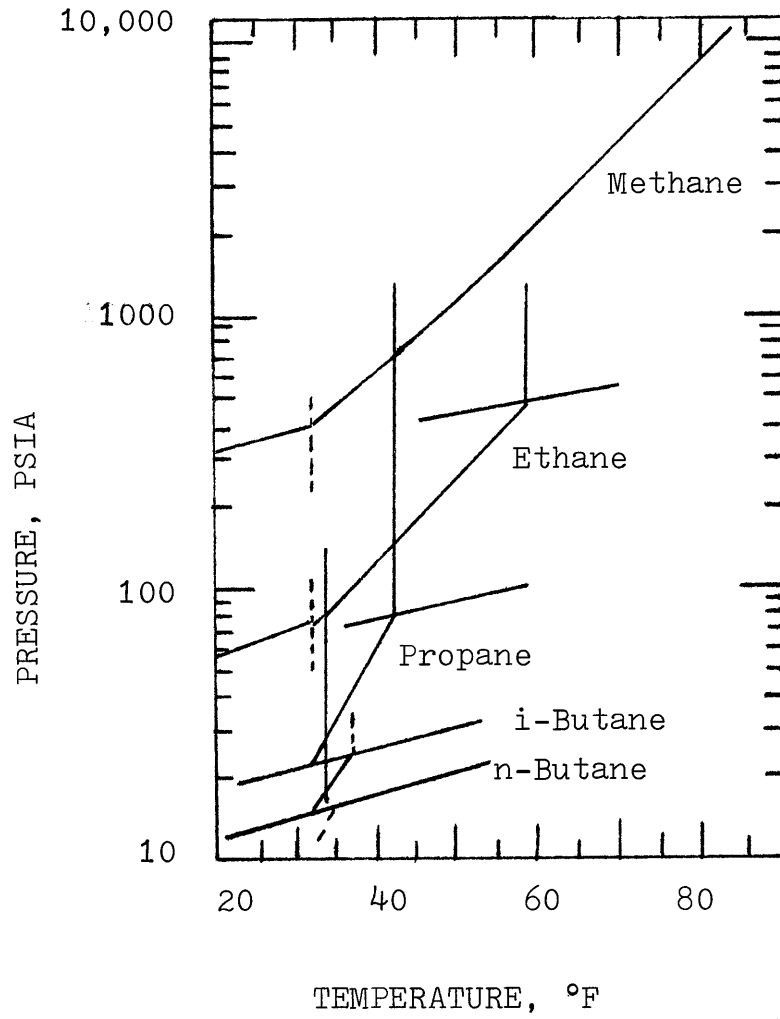
Fig. $\dfrac{6}{----}$

Hydrate-Forming Conditions For
Paraffin Hydrocarbons
(Katz et al., 1959)

The mechanisms for hydrate formation is not understood, but it is obvious that subcooling of the water-gas mixtures below 0°C is not necesary. The low solubility of hydrocarbons in water, and hydrate generation in a gas supersaturated with water initiated at solid surfaces, suggest that the process is a surface phenomena and not a bulk water process.

CHAPTER 3: EXPERIMENTAL

3. EXPERIMENTAL

In all experiments, the liquid cryogen was boiled on a water surface. The boiling vessel was made of polysterene as illustrated in Figure (7). In the front wall there was inserted two sheets of acrylic plastic material, each 2 mm in thickness, with 0.9 cm separation. Nitrogen was passed between three sheets before an experiment to elimiate condensation on the front wall. The inside walls were covered by thin sheets of polyacetate to prevent leaks. The dimensions of the vessel were: length 25 cm, width 17.3 cm, and dept 7.5 cm, the water surface area was 129.75 cm^2.

In front of the vessel was located the high speed motion picture camera, and illumination was obtained from three high intensity 500W spot lights. At the top of the container was a portable hood which was connected to the main hood in the laboratory to prevent any accumulation of hazardous vapors.

In each run, there was 10 cm of water at room temperature. High speed movies were taken at different camera speeds, but the distance of the camera to the front wall of the vessel was always the same.

The LNG composition was expressed on a mole per cent basis and mixtures were always within the range of no possible

55

HOOD

LNG

7.5 cm

0.9 cm

25 cm

12 cm

H_2O

17.3 cm

CAMERA
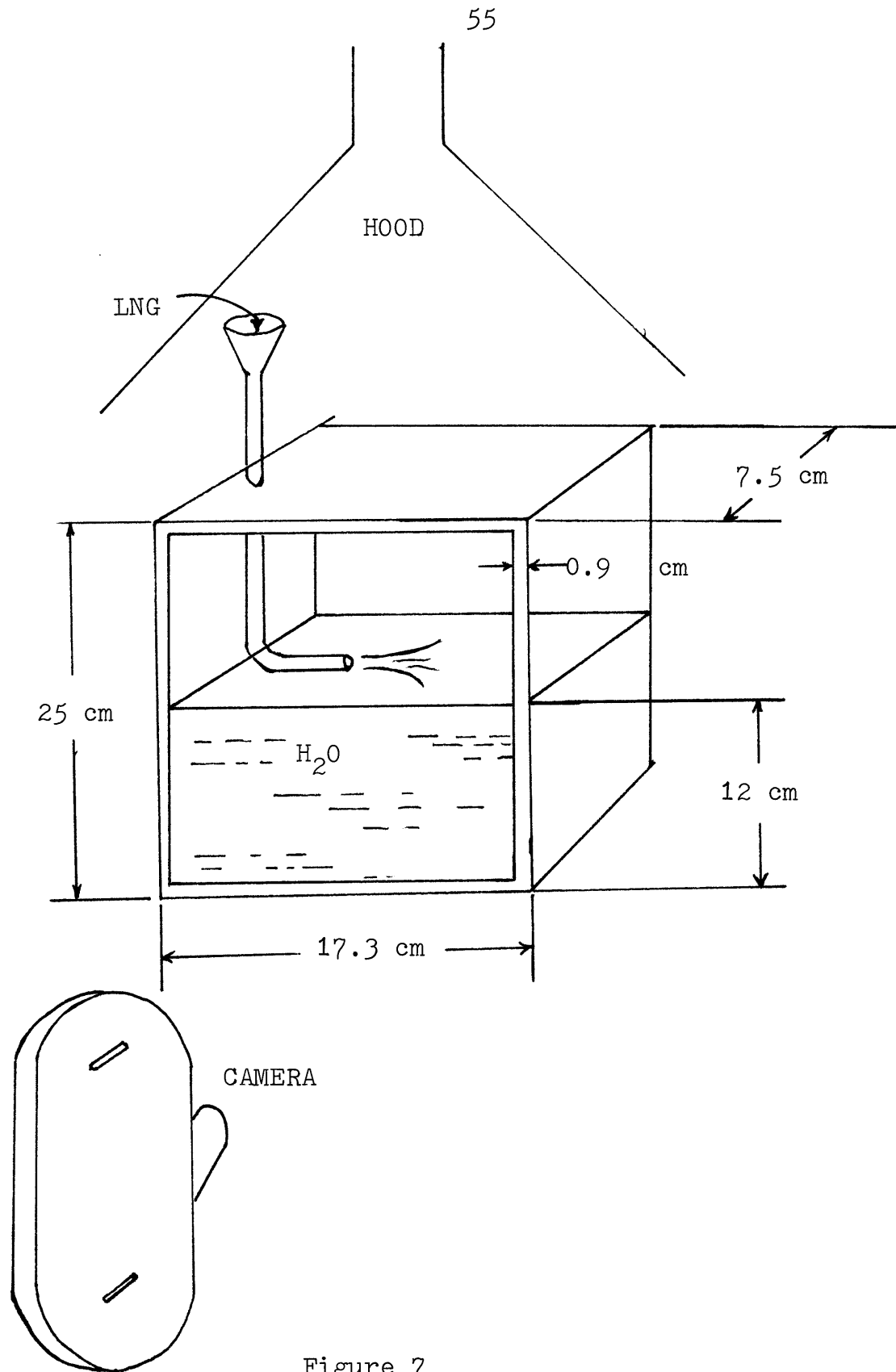
Figure 7

flameless-vapor explosions. In preparing mixtures rich in methane, the Dewar was precooled to temperatures equal to or slightly lower than the bubble points of the test liquid. This minimized any change in the liquid composition before and during discharge onto the water. Splashing was avoided making the liquid cryogen run down by a funnel which ended in a U-shape so the contact angle with the water surface was at a minimum.

The mixtures were always made with methane of CP grade having a composition of 99.5 % of methane, 0.3 % ethane, 0.1 % propane, 0.05 % butane. Ethane and propane CP grade were used, (these gases had a trace of heavier hydrocarbons in their composition). Methane of ultra high purity was used to demonstrate that foam is a characteristic of mixtures and that with pure liquids foam does not form.

3.1 RESULTS

Table no. 2	1	2	3	4	5	6	7
Composition							
% N_2							
% Methane	100			99.9	99.9	99	99
% Ethane		100					
% Propane			100		0.1		1
% Butane				0.1		1	
Mass Spilled, g	150	150	140	160.4	160.2	164.2	146.5
Camera Speed, fps	100	100	300	100	100	100	100
General Description of Boiling*	V	A-Q	VV	V	V	VV	VV
Bubble							
Bimodal	x	x		x	x	x	
Large Size Range, cm	1-1.5	1-2		2-4	1-2	1-2	
Small Size Range, mm	2-3	1-3		2-4	1-2	1-2	
Unimodal Size Range, mm							3-5
Foam							
Description							
N/P/D**	D	N	N	D	D	P	P
R/C/W***	W			W	R	R	R
Duration, s	20			20	20	30	30
Height, cm	5			5	8	15	15
Ice							
Forms rapidly	yes	yes	yes	yes	yes	yes	yes
Perforations	yes	no	no	yes	yes	no	yes

57

Continuation Table no. 2	8	9	10	11	12	13	14
Composition							
% N_2		1				5	
% Methane	99	99	95	95	95	95	93
% Ethane	1				5		5
% Propane				5			2
% Butane			5				
Mass Spilled, g	145.3	161.2	181	156.6	150.3	176	155
Camera Speed, fps	100	100	100	100	100	100	200
General Description of Boiling*	V	V	VV	VV	VV	V	VV
Bubble							
Bimodal	x	x		x		x	
Large Size Range, cm	2-3	3-5		1-3		2-4	
Small Size Range, mm	1-2	1-3		2-5		1-3	
Unimodal Size Range, mm			1-2		1-3		1-2
Foam Description							
N/P/D**	P	P	P	P	P	D	P
R/C/W***	R	C.R	R	R	R	C.R	R
Duration, s	20	10	10	20	20	30	20
Height, cm	10	6	15	15	15	10	15
Ice							
Forms rapidly	yes	yes	yes	yes	yes	no	yes
Perforations	yes	yes	yes	no	yes	yes	no

58

Continuation Table No. 2	15	16	17	18	19	20	21	22
Composition								
% N_2							99	95
% Methane	87	85	84	80	60	5		5
% Ethane	9	10	16	11	25	95		
% Propane	4	5		9	15		1	
% Butane								
Mass Spilled, g	113	187.1	154.9	140	189.6	383.2	281.6	274
Camera Speed, fps	200	100	200	100	200	100	100	100
General Description of Boiling*	V	VV	VV	V	V	A-Q	V	Q
Bubble								
Bimodal	x		x	x		x	x	x
Large Size Range, cm	3-5		1-2	2-4		0.5-1	2-3	1-2
Small Size Range, mm	10-20		1-2	1-3		1-2	1-3	1-2
Unimodal Size Range, mm		1-2			1-2			
Foam								
Description								
N/P/D**	P	P	P	P	P	N	N	P
R/C/W***	W	R	R	R	W			CR
Duration, s	10	25	30	10	20			30
Height, cm	3	15	15	6	5			10
Ice								
Forms rapidly	yes	yes	yes	yes	yes	yes	no	no
Perforations	yes	no	no	no	yes	no		

59

*Boiling

      A: Active

      Q: Quite

      V: Violent

      VV: Very violent

**Foam

      N: None

      P: Promptly

      D: Delay

***

      R: Reach

      C: Creamy

      W: Weak

3.2 DISCUSSION

One of the main objectives of this thesis was to conduct
a careful, detailed and accurated experimental study of the
foaming phenomena that is present when a spill of LNG occurs
on a pool of water. In order to accomplish this objective,
the set-up showed in Figure (7) was designed and with the
help of the Hycam (High speed motion picture camera) the
complete analysis of each run or test was made. These results
were shown in the preceeding tables in which each test was
analysed frame by frame.

Photographs were taken from the movies, the pictures
obtained provided valuable information relative to ice forma-
tion, foam and bubble sizes. A few selected time-sequenced
pictures of the cryogen-water interface are presented in
Figures   -   Pictures are full-sized unless noted other-
wise.

The following set of photographs show a time-sequence
events of what occurs when 100% methane (CP grade) is poured
onto water.

In Figure (8) the view of the vessel is shown before
the LNG is poured, it is noted the water surface above the
rule and almost at the same level as the end of the funnel.
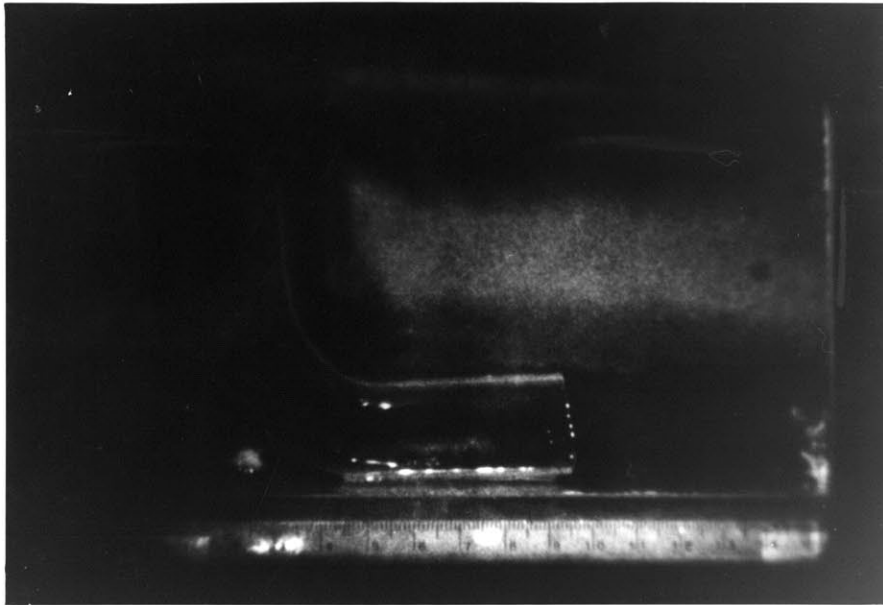
Figure 8

View of the vessel before the LNG is
poured. It is to be noted that the
water surface is above the ruler (cm
scale)

Figure   9

A typical picture of the first second
of LNG boiling on water when the mix-
tures are rich in methane, 99 % or
more.
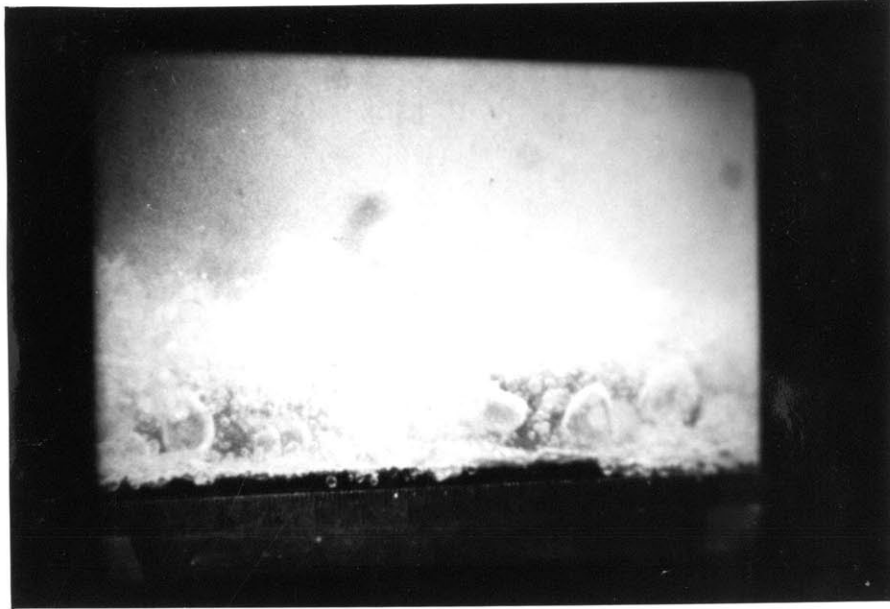
Figure 10

Three seconds later, after picture 2,
it is noted the bubbles size is de-
creasing at the bottom.

Figure 11

At the 10th second of the run, foam-
ing is taking place. It has reached
a height of 4 cm. Note the bubble
size distribution.

Figure 12

At the 18th second, the foam reached
its maximum height from 5 to 6 cm.

Figure 13

At the 20th second, foam starts break-
ing down. Note the big bubbles at the
top left corner.

Figure   14

At the 35 second, foam is decreasing
with some vapor bubbles explosions.
Note the vapor clouds.

Figure 15

At the 40 second, foam height has been
reduced in level more than half and it
is decreasing very rapidly.

The photographs shown in Figures (8 - 15), illustrate the surface between 100% methane and water. A significant point to be noted is the extraordinary rapidity with which the ice layer is formed at the water surface. In the first second or so, bubbles form and fog is noted. Bubbles grow at a very fast rate without coalescing, therefore, the foam becomes evident.

In tests number 5, 6, 10, 11, 12, 14, 16, and 17 the foam reached the top of the container (which is 15 cm high) and in some of them, it overflowed the container. The common characteristic of these tests was the high concentration of methane in the mixture (90% or more), except in tests number 16 and 17 where the concentration in methane was lower (85% and 84% respectively), but in both of these, there was a high concentration of ethane (10% and 16% respectively). A common and interesting feature is that the boiling of all these mixtures was violent, and the bubble size was always in the bimodal distribution range with the big bubbles in the range from 1 to 2 cm, and the small ones in the range from 1 to 2 mm. In some cases, as in tests number 10, 12, 14, and 16 the bubble size was uniformly distributed in the range of the small bubbles (from 1 to 2 mm).

An average foam life for these tests is 23 seconds; it varies from 10 seconds (in test number 11) to 30 seconds (time reached in tests number 6, 10 and 17).

The following set of time-sequenced pictures show a characteristic test of these extremely violent boiling mixtures when the foam overflows the container in less than a second after the LNG was poured onto the water surface. The photographs were taken from test number 10, which has a composition of 95% methane and 5% butane.
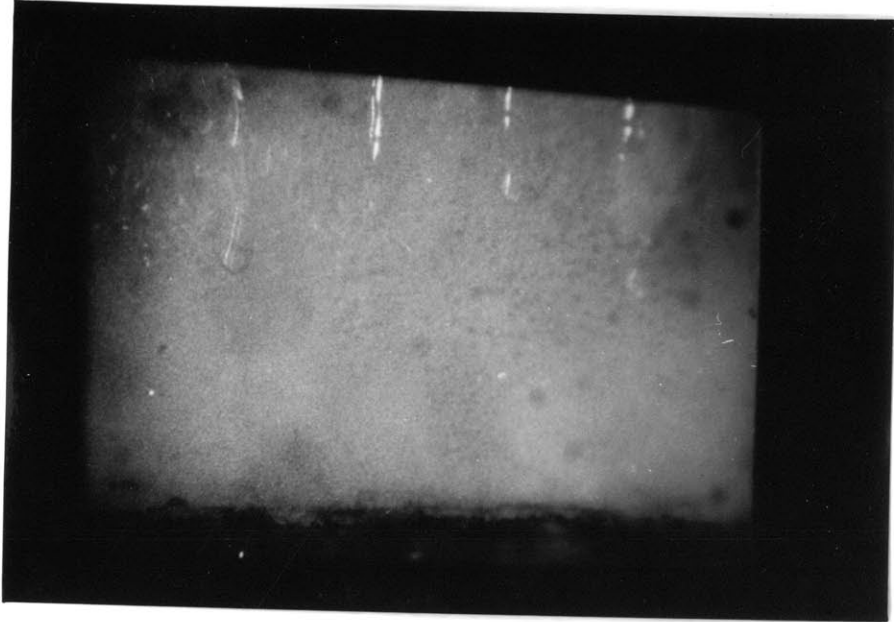
Figure   16

At the first second of the run, foam
has overflowed the container. Liquid
LNG is noted in the outside wall.
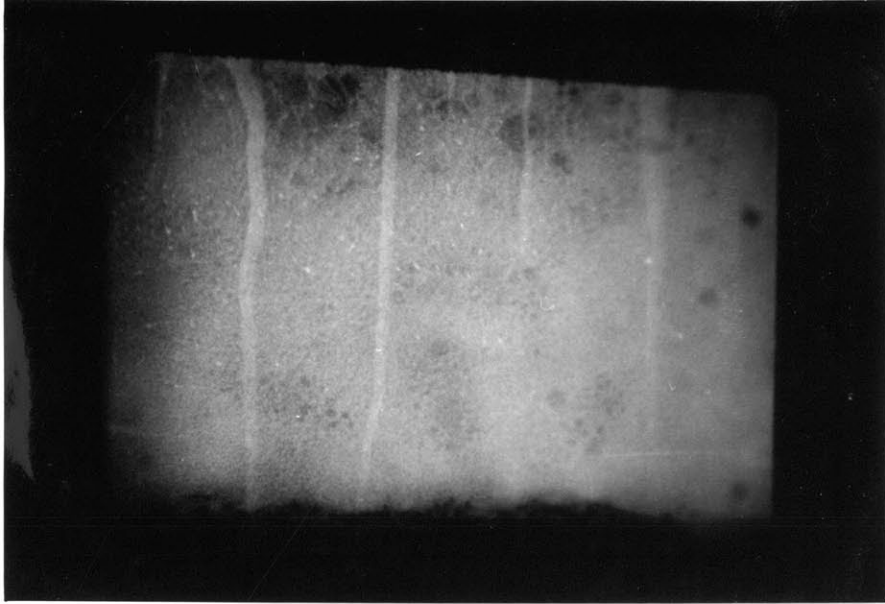
Figure 17

At the second second of the run, foam
still at the top of the container.
Note the liquid column of LNG frozen
on the outside wall.
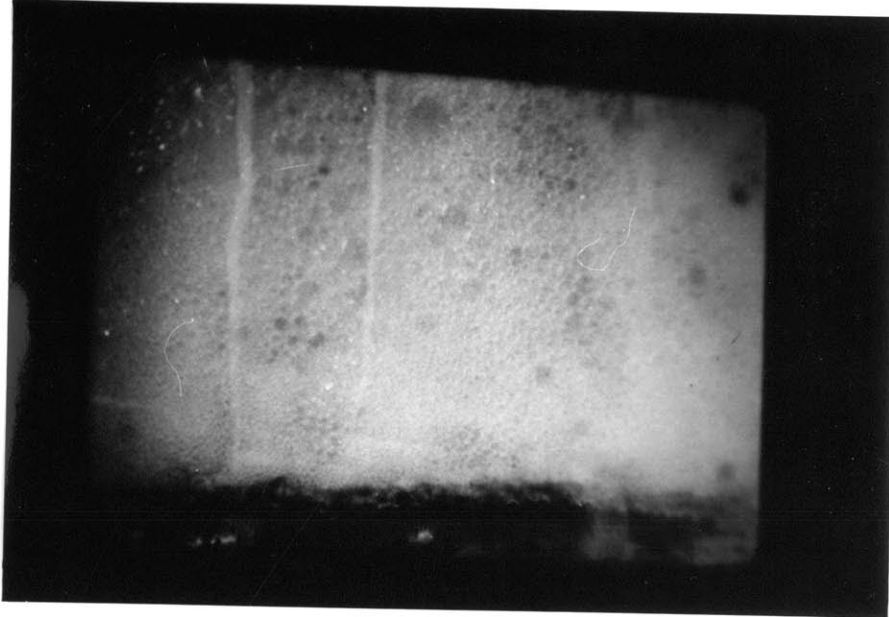
Figure   18

At the 10th second of the run, foam
still on top of the container, but
it is starting to break down. Note
the big bubbles formed at the top
left corner.
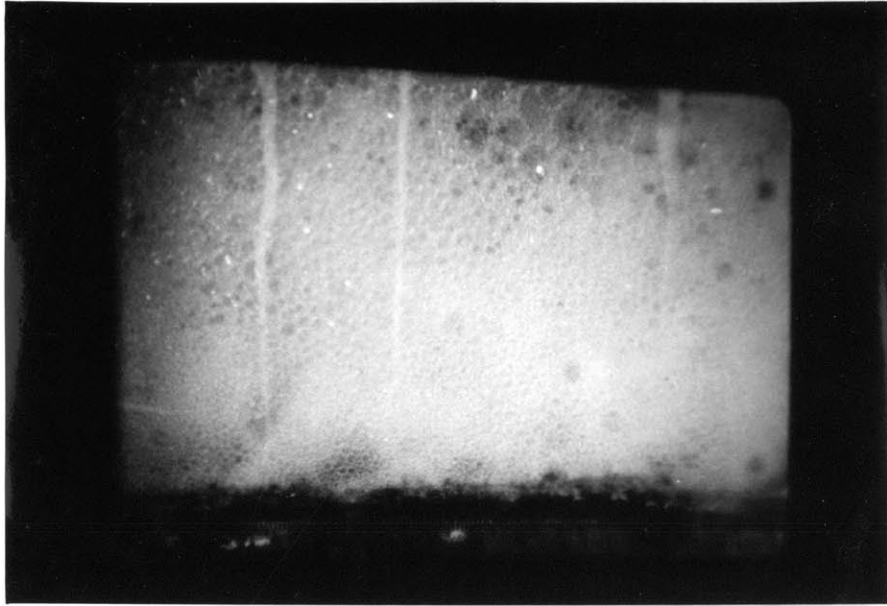
Figure   19

One second later, at the 11th second,
foam is breaking down. Note the big
bubbles formation at the top.

Figure   20

At the 12th second, the bimodel size
distribution of bubbles is clearly
differentiated.

Figure   21

Between the 13th and 14th seconds,
foam has decreased in level. There
are liquid deoplets in the inside
wall of the container.

Figure   22

At the 14th second, foam keeps de-
creasing rapidly.   There are vapor
clouds and severe turbulence at the
top left corner.

Figure   23

At the 20th second of the run, foam
still evident. more liquid droplets
and vapor clouds appear at the top.

In tests number 5, 8, 9, 13, and 18 the foam reached a height of at least 6 cm but it never exceeded 10 cm. Once more, we have a mixture very rich in methane (99% and more), except in test number 13 (95% methane), and test number 18 (80% methane). The characteristics are the same for all the tests. Boiling was violent, the bubbles size distribution was always bimodal in the range of big bubbles from 2 to 4 cm, and small ones from 1 to 3 mm. Foam-life time-average for these tests is 18 seconds. In test number 1, 4, and 19 the foam formation only reached 5 cm of height. The common characteristic for tests 1 and 4 was the high percentage of methane and in test 19 the low percentage in methane. Test 1 was 100% methane CP grade which contained impurities (traces of heavy hydrocarbons), and test number 4 was 99.9% methane and 0.1% butane; in both tests the foam formation occurred with a delay of few seconds, the big bubbles formed first, as in Figure (8). Later in the run, it was observed that the small bubbles formed a consistent foam for a period of 20 seconds. In test number 19 the composition was 60% methane, 25% ethane, and 15% propane; the only difference in the results of these tests with tests 1 and 4 is that the foam occurred sooner, but it was of the same consistency and it lasted for the same period of time (20 seconds). In all of these tests the

foam formation was weak and the ice formation occurred instantaneously.

In tests number 2, 3, 20, and 21 no foam formation occurred. In tests 2 and 3 (100% ethane and 100% propane respectively), the ice formation took place immediately and the cryogen boiled off very quitely. In test 21 (99% nitrogen and 1% propane), no ice formation occurred. In test 22 no ice formation occurred either, but foam was creamy and rich, foam lasted for a period of 30 seconds and it reached a height of 10 cm.

The principal value of these pictures is to estimate the bubble sizes. It appears that the small bubbles reside in the cryogenic liquid, Figure (17), held to the cryogen lower free surface by surface tension forces. It is believed that these small bubbles produced only at the beginning of the runs with LNG, coalesce to a size large enough for buoyancy forces to disengage them into the bulk cryogen. Consequently, the quantity of the small bubbles decays rapidly. Few small bubbles are visible in Figure (15), 20 seconds into the run. The small bubbles are responsible for the extension <u>foams</u> observed above boiling positive liquid mixtures such as LNG (i.e., those mixtures in which the most volatile component

has the lower surface tension). In Figure (24), surface
tension data for ethane and other higher alkanes have been
extrapolated to 161.5°C (the b.pt. of CH_4) for comparison
purposes. Burgess et al. (1970) observed foaming above
boiling LNG pools, Van Wijk and Van Stralen (1956), and
Hovestreijdt (1963) also reported that they observed <u>foams</u>
above boiling positive liquid mixtures.

The origin of the small bubbles is not exactly under-
stood, but it may be related to the activities as soon as
a cryogenic liquid mixture is contacted with a hot surface,
water in the present studies. The first vapors produced
from a typical LNG, probably by heterogeneous nucleation at
the cryogen-heating medium interface, will be almost pure
methane. The depletion of this volatile component at the
liquid wall surrounding the vapor causes a concentration
gradient to exist, <u>both</u> between the bubble surface and bulk
liquid, <u>and</u> along the bubble walls, i.e., the concentration
of methane at <u>a</u> is less than at <u>b</u> which, in turn, is less
than at <u>c</u> (Figure 25). The latter implies that a surface
tension gradient should exist at the wall, and surface tension
induced liquid motion (Marangoni* effect) should occur from

-----
*The induced flows are commonly known as the"Marangoni" effect.
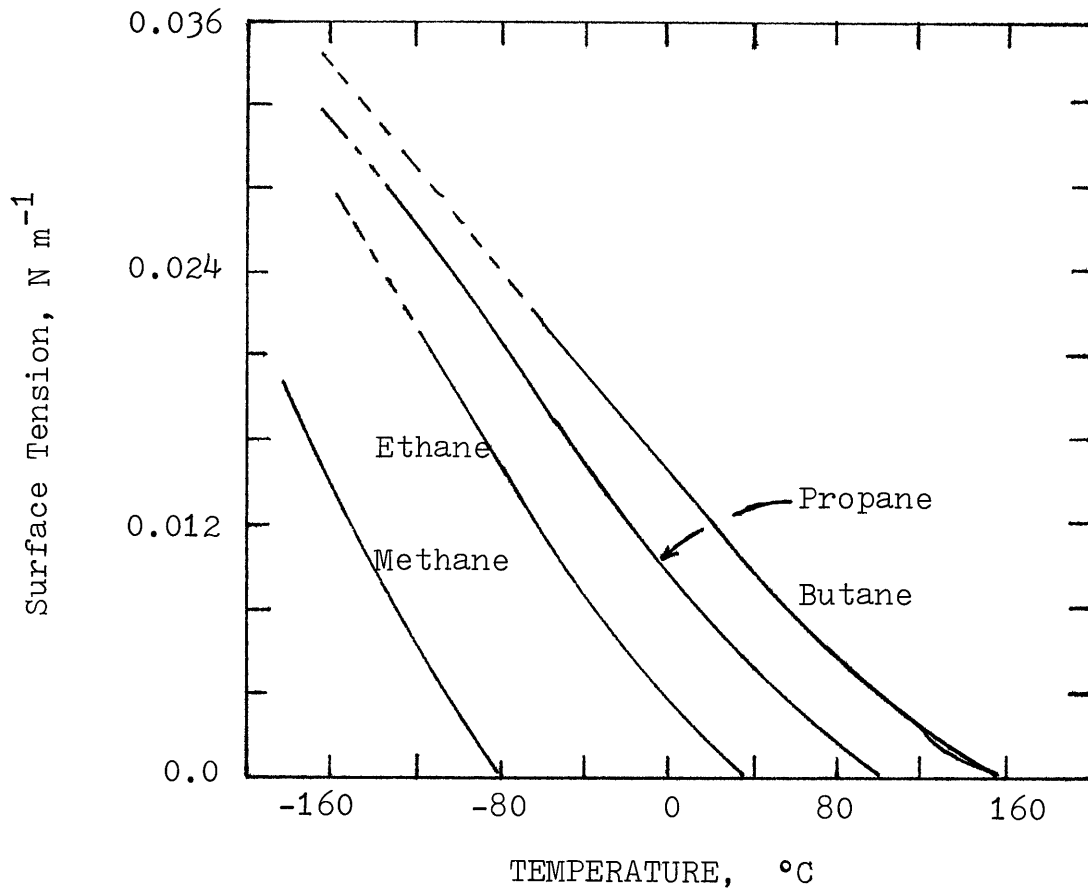
Fig. _24_
Surface Tension vs. Temperature For
Cryogenic Hydrocarbon Liquids.
(Gallant, 1968)

site b to site a, in the sketch below.   An upward drag force
is, therefore, exerted on the bubble.
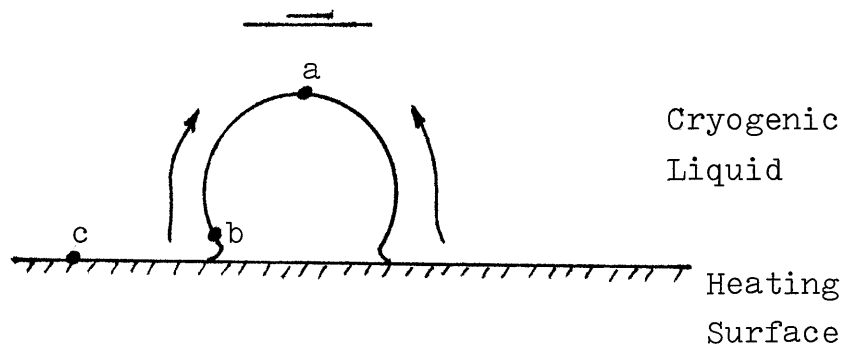
Figure   25

Thus acting on the bubble are buoyancy, inertia and drag
forces (assisting bubble growth) and surface tension (resist-
ing deformation).   The relative magnitude of these forces de-
termine whether the bubbles will grow to big sizes and be de-
tached into the bulk cryogen, form small bubbles which may be
retained near the interface, or revert to a flat surface.   In
a rapidly growing bubble, the effective bubble wall surface
tension increased with time.   It is postulated here that small
bubbles become pinch-off (to minimize surface area) when the

effective surface tension force overtakes the net growth assisting force and the bubble shape is similar to, or more developed than shown in the sketch. Moreover, if the pinching-off process is sufficiently rapid, and the buoyancy force on the bubble formed is low, surface tension will stabilize the bubble at the interface.

This model is in effect a combination of the bubble growth slowing-down process proposed by Van Wijk and Van Strahlen (1956), and the Marangoni effect proposed by Hovestreidjt (1963).

The events, just described, occur rapidly, before the cryogen is separated from the heating surface (water) by a vapor film, as Figure (15) suggests. With large ΔT across the liquids, no new small bubbles are believed generated after this initial period, unless where the liquids touch again. Another mechanism can be postulated that as soon as the liquids contact, the cold liquid becomes superheated in a zone next to the interface. Then homogeneous nucleation of small bubbles takes place within this layer or zone. This is reasonable, except that it implies that small bubbles should be generated within pure methane as well as in LNG contacted with water. The small bubbles, were not obtained with pure cryogenic liquids as much as with LNG.

3.2.1   CORRELATION FOR BUBBLE DIAMETERS

A model of a bubble node in static equilibrium, as shown below, is subjected to two primary forces; buoyancy and the surface tension forces.

Model of Bubble in Film Boiling
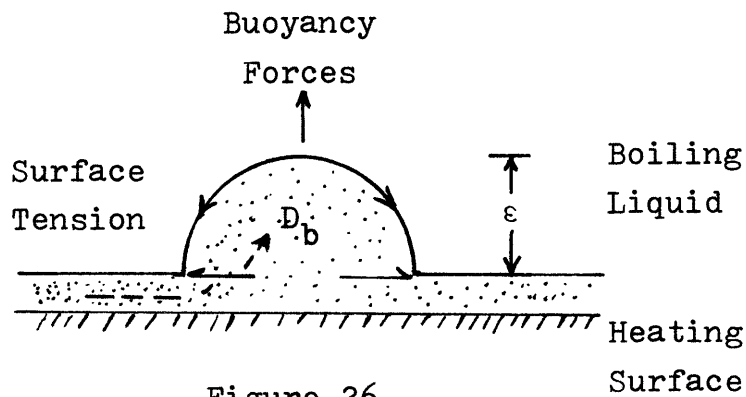
Figure 26

The force balance equation is given by

$$V_b \; g \; (\rho_L - \rho_v) \; = \; \pi \, D_b \, \sigma \qquad (27)$$

where the node volume, V_b , can be related to the diameter, D_b , with the expression, experimentally established by Borishansky (1959), i.e.,

node height, $\varepsilon \; = \; 0.68 \, D_b$ $\qquad (28)$

Equation (27) then becomes

$$D_b = \Phi \sqrt{\frac{\sigma}{g(\rho_L - \rho_v)}} \qquad (29)$$

where Φ is 2.8.

In the boiling processes of this study, however, bubbles were observed to grow so rapidly that additional forces, such as inertia, pressure and drag forces, should be taken into account in any analysis. Since the data for quantitizing some of these forces are unavailable, prefactor, Φ , (Equation 29) has been computed from experimental data and is presented in Table 3.

The average value of Φ for the cryogenic hydrocarbon liquid is 7.7. Hence, the bubble sizes are correlated with the following expression

$$D_b = 7.7 \left[\frac{\sigma}{g(\rho_L - \rho_v)}\right]^{1/2} \qquad (30)$$

(Equation 30) is strictly valid for the experimental contiditions of this study. It is conceivable, though that the range of application may be broader.) As shown in the table, the prefactors obtained here are larger than presented by Berenson (1961) for boiling hydrocarbons near the Leidenfrost point. This is consistent with the fact that larger bubbles are observed in this study than reported by him. The high

TABLE 3

VALUES OF THE PREFACTOR Φ (EQUATION 29) FOR DIFFERENT SYSTEMS

System	$\pm$ 10%
Liquid nitrogen - glass	7.0
Liquid nitrogen - water	8.12
Liquid methane (99.98%) - water	7.6
Liquid ethane (99.85%) - water	7.78
n-Pentane - ; Carbon tetrachloride - metallic surfaces (Berenson, 1961)	4.7
Static equilibrium	2.8

values of Φ are also evidence of the departure from the static equilibrium situation.

CHAPTER 4: CONCLUSIONS AND RECOMMENDATIONS

4.   CONCLUSIONS AND RECOMMENDATIONS

The conclusions of this work are summarized as follows:

1. With pure liquid methane, the bubbles were large and no foam was present, whereas for LNG, there was a distribution of bubbles sizes with many that were very small, they did not coalesce and produced a rich and consistent foam.

2. A bimodel size distribution of bubbles was observed in the spills of rich LNG mixtures, the range was from 2 to 4 cm for the big bubbles, and from 1 to 3 mm for the small ones.

3. Boiling was very violent for specific tests of the experimental part of the thesis, in such cases the production of small bubbles was increased and the "foam" formation reached its maximum height of 15 cm and more.

4. In some cases, the formation of foam occurred with a delay of a few seconds. The life-time of the foams obtained in this work varied from 10 seconds to 30 seconds.

5. In pure methane, ethane, and propane, there was no foam formation, neither was there foam in compositions with high concentration of liquid nitrogen (99% or more).

6. Ice formation took place rapidly on the water surface in all the spilles except the ones that contains a high concentration of liquid nitrogen (95% or more).

It is recommended that continuing research include examination of the following points:

1. The surface tension of binary mixtures of methane and the higher alkanes should be determined as a function of liquid composition (at the equilibrium temperatures). Both static and dynamic surface tension values should be established if possible. This should permit a better understanding of small bubble production in positive liquid mixtures.

2. Formation of hydrates by cold hydrocarbon gases should be studied. The conditions of hydrate formation above a water surface at low vapor temperatures and pressures should be established.

3. The turbulence at the water surface should be closely examined for its efficiency of ice particle recirculation.

There is still a great deal to be learned about the mechanism when cryogenic hydrocarbon mixtures boil on water.

In continuing research, the processes of ice nucleation
and growth, and flows within the water, especially near
the interface should be investigated.

APPENDICES

APPENDIX   A

EXPERIMENTAL RESULTS

RUN No. 1

Spill of Methane on water

Composition: 100 % methane CP grade

Mass spilled: 150 g

Volume spilled: 333.3 cm^3

Film: Tri - X Reversal 7278   100 ft   Focus 8   ASA 160

Camera speed: 100 F.P.S

Time elapsed: 40 s

As soon as the spill was made violent boiling was observed.
During the first five seconds a bimodel size distribution of
bubbles was formed, with the large bubbles a size from 1 to 1.5
cm and the small ones from 2 to 2 mm. Foam appeared to form
rapidly and reached a height of 5 cm with little coalescing.
The foam lasted for about 20 seconds after which time it start-
ted to decrease in height. Ice formation occurred during the
first three seconds. Perforations were visible in the ice.

RUN No. 2

Spill of ethane on water

Composition: 100 % ethane

Mass spilled: 150 g

Volume spilled: 333.3 cm^3

Film: Tri - X Reversal 7278 100 ft Focus 8 ASA 160

Camera speed: 100 F.P.S.

Time elapsed: 40 s

Violent boiling was observed with formation of both
large bubbles (1 to 2 cm in diameter) and small bubbles (1 to
2 mm). There was no foam. Ice formation occurred within the
first 3 seconds with a fine thickness of 1.5 cm and no perfo-
rations.

RUN No. 3

Spill of propane on water.

Composition: 100 % propnane

Mass spilled: 50 g

Volume spilled: 111.1 cm^3

Film: 4 - X Reversal 7277 100 ft Focus 8 ASA 320

Camera speed: 300 F.P.S.

Time elapsed: 10 s

In this run the funnel was not used and when the propane impacted the water from a height of 18 cm, a splash was observed with violent and explosive boiling. Ice formed instantaneously and there were no bubbles formed; therefore, no foam. Evaporation was completed in less than a second.

A second run with 140 grams of propane was made using the funnel. Again ice formed very rapidly, after which time the propane boiled quietly with no foam formation.

RUN No. 4

Spill of LNG on water

Composition: 99.9 % methane

0.1 % butane

Mass spilled: 160.4 g

Volume spilled: 356.2 cm^3

Film: Tri - X Reversal 7778   100 ft   Focus 11   ASA 160

Camera speed: 100 F.P.S.

Time elapsed: 40 s

During the first 20 seconds of the experiment vigorous boiling was noticed; bubbles were formed with diameter from 2 to 4 cm, no foam was observed and the ice had a thickness of 2 cm with some big perforations.

After 20 seconds, consistent foam started to develop and reached a height of 5 cm with small bubbles from 2 to 4 mm. It lasted for a period of 20 seconds.

RUN No. 5

Spill of LNG on water

Composition: 99.9 % methane

0.1 % propane

Mass spilled: 160.2 g

Volume spilled: 356.17 cm^3

Film: Tri - X Reversal 7278   100 ft   Focus 11   ASA 160

Camera speed: 100 F.P.S

Time elapsed: 40 s

Violent boiling was observed with the same characteristics of the spill of 100 % methane C.P. grade. A bimodel distribution of bubbles was noted with sizes from 1 to 2 cm, and from 1 to 2 mm. Foam appeared 5 seconds after the spill was made and reached a height of 8 cm. It decreased with time but remained consistent for the following 20 seconds. At the end, the small bubbles increased their diameter but still formed a foam. The ice layer was from 1 to 1.5 cm thick with one big perforation.

RUN No. 6

Spill of LNG on water

Composition: 99 % methane

                 1 % butane

Mass spilled: 164.2 g

Volume spilled: 362 cm^3

Film: Tri - X Reversal 7278   100 ft   Focus 11   ASA 160

Camera speed: 100 F.P.S

Time elapsed: 40 s

    Exceptionally violent boiling was noted. The bimodel
distribution size of bubbles was from 1 to 2 cm for the big
bubbles, and from 1 to 2 mm for the small ones. The small
bubbles were uniformely distributed and formed a rich foam
that overflowed the container during the first few seconds.
Then, it decreased in height very slowly but kept its con-
sistency for more than 30 seconds. The ice formation was
from 1 to 2 cm thick and had no perforations at all.

RUN No. 7

Spill of LNG on water

Composition: 99 % methane

                1 % propane

Mass spilled: 146.5 g

Volume spilled: 325 cm^3

Film: Tri - X Reversal 7278   100 ft   Focus 11   ASA 160

Camera speed: 100 F.P.S

Tiem elapsed: 40 s

   A tremendous violent boiling occurred immediately after
the spill of LNG was made with very vigorous foam formation
with a height in excess of 15 cm.   It was very consistent for
a period of time of 30 seconds and then decreased.   The size
of the bubbles was always from 3 to 5 mm and the ice was 2 cm
thick with big perforation in it.

RUN No. 8

Spill of LNG on water

Composition: 99 % methane

                1 % ethane

Mass spilled: 145.3 g

Volume spilled: 322.8 cm^3

Film: Tri - X Reversal 7278   100 ft   Focus 8   ASA 160

Camera speed: 100 F.P.S

Time elapsed: 40 s

Very vigorous boiling with a bimodel distribution of
bubbles size took place immediately. The big bubbles with a
size from 2 to 3 cm in diameter were at the water surface, and
the small ones with a diameter from 1 to 2 mm formed a very
consistent foam which reached a height of 10 cm during the
first 20 seconds. Foam then decreased very rapidly. The
ice formation was of 1.5 cm thick with only one big perfora-
tion and 3 to 4 small ones. In some spots the ice layer was
very thin.

RUN No. 9

Spill of LNG on water

Composition: 99 % methane

                1 % nitrogen

Mass spilled: 161.2 g

Volume spilled: 358.12 cm^3

Film: Tri - X Reversal   100 ft   Focus 5.6   ASA 160

Camera speed: 100 F.P.S

Time elapsed: 40 s

During the first 25 seconds of the experiment, an ex-
tremely violent boiling was noted but little foam. The bubbles
distribution was of big sizes from 3 to 5 cm with very few
small ones. The formation of the ice layer occurred with a
delay of few seconds.

After the first 25 seconds, the bubbles decreased in diam-
eter from 1 to 3 mm and the foam formed reached a height of 6
cm for a period of time of 10 seconds. The ice formation had
a thickness from 1 to 2 cm with big perforations throughtout
the surface.

RUN No. 10

Spill of LNG on water

Composition: 95 % methane

                  5 % butane

Mass spilled: 181 g

Volume spilled: 382.2 cm^3

Film: Tri - X Reversal 7278 100 ft Focus 11 ASA 160

Camera speed: 100 F.P.S

Time elapsed: 40 s

    Extremely violent and explosive boiling. The foam forma-
tion took place immediately with small bubbles size from 1 to
2 mm. During the first 5 seconds the foam reached the top of
the container with a height of 15 cm and it overflowed the
container. The foam rate decreased slowly with time but it
remained consistent for the following 20 seconds. As the foam
decreased, small vapor explosions were observed at certain
spots of the surface, and as the foam disappeared, the LNG
kept boiling very quietly with a height of 1 cm. The ice
formation was of 1 cm thick with very thin layers.

RUN No. 11

Spill of LNG on water

Composition: 95 % methane

5 % propane

Mass spilled: 156.6 g

Volume spilled: 350 cm^3

Film: Tri - X Reversal 7278   100 ft   Focus 8   ASA 160

Camera speed: 100 F.P.S

Time elapsed: 40 s

Very vigorous and violent boiling. The bimodel distribution of bubbles size was clearly observed, being the big ones from 1 to 3 cm in diameter and the small ones with the particularity that they were larger in diameter (3 to 5 mm) than in the past experiment (1 to 2 mm). Significant foaming was noted with a height of 15 cm but it only lasted for a short period of time of 10 seconds and decreased at a very fast rate with many vapor explosions which caused that very dense vapor clouds were formed. The ice formation was of 2 cm thick with no perforations at all, although in some parts of the ice layer it was very thin and transparent.

RUN No. 12

Spill of LNG on water

Composition: 95 % methane

                5 % ethane

Mass spilled: 150.3 g

Volume spilled: 334 cm^3

Film: Tri - X Reversal 7278   100 ft   Focus 8   ASA 160

Time elapsed: 40 s

Camera speed: 100 F.P.S

    Very vigorous boiling. The foam reached the top of the container (15 cm). Small bubbles from 1 to 3 mm were noted. It was observed in the motion picture movie that a few drops of the mixture came out of the container during the first 10 seconds. After 20 seconds the foam was reduced in level very rapidly until it disappeared and the ethane boiled quietly. Ice formation took place immediately and was uniform with a thickness from 1.5 to 2 cm and few small perforations.

RUN No. 13

Spill of LNG on water

Composition: 95 % methane

                5 % nitrogen

Mass spilled: 176 g

Volume spilled: 355.2 cm^3

Film: Tri - X Reversal 7278   100 ft   Focus 8   ASA 160

Camera speed: 100 F.P.S

Time elapsed: 40 s

As the mixture was poured onto the water, the boiling got vigorous and violent, and eventhough the bimodel size distribution of bubbles was present, there was no foam formation during the first 10 seconds. The big bubbles were from 2 to 4 cm in diameter, and the small ones from 1 to 3 mm. It was remarkable the similitude of this experiment to the one of the spill of methane CP grade during the first 10 seconds. After this period of time, the foam started to develop at a very fast rate. It reached a height of 10 cm for 30 seconds. The ice layer was formed with a delay of a couple of seconds. It had a thickness of 2 cm with some small perforations.

RUN No. 14

Spill of LNG on water

Composition: 93 % methane

5 % ethane

2 % propane

Mass spilled: 155 g

Volume spilled: 345 cm^3

Film: Tri - X Reversal 7278   100 ft   Focus 5.6   ASA 160

Camera speed: 200 F.P.S

Time elapsed: 20 s

Very vigorous boiling was observed. The foam formation took place immediately after the spill of LNG was made with small bubbles formation from 1 to 2 mm in diameter. The foam reached a height of 15 cm which lasted 15 seconds, then it reduced its level about half. Ice formation was 2 cm thick with some peacks that reached 4 cm. After the foam disappeared the LNG kept boiling quietly for 3 minutes.

RUN No. 15

Spill of LNG on water

Composition: 87 % methane

                9 % ethane

                4 % propane

Mass spilled: 113 g

Volume spilled: 250 cm^3

Film: 4 - X Reversal 7278   200 ft   Focus 8   ASA 320

Camera speed: 200 F.P.S

Time elapsed: 40 s

Vigorous boiling was noticed with a bimodel size distribution of bubbles, the large ones were bigger than normal (from 3 to 5 cm). The presence of very dense vapor clouds did not permit to delineate the size of the small bubbles. When the vapor clouds dissipated, the height of the foam had already decreased to 3 cm. The LNG kept boiling less vigorous. The foam lasted for a period of time of 10 seconds, then it was clearly observed how at this stage the bubbles size was uniformely distributed at the top layer of the boiling LNG (from 10 to 20 mm in diameter), and with vapor bubbles explosions. Ice formation was from 1 to 1.5 cm thick with few big perforations. It was possible to observe the turbulence under the ice layer.

RUN No. 16

Spill of LNG on water

Composition: 85 % methane

10 % ethane

5 % propane

Mass spilled: 187.7 g

Volume spilled: 417 cm^3

Film: Tri - X Reversal 7278 100 ft Focus 4 ASA 40

Camera speed: 100 F.P.S

Time elapsed: 40 s

Exceptionally violent boiling was observed as soon as the LNG impacted the water. Because of the type of film used in this experiment, the bimodel size distribution of bubbles was impossible to measure, althoug the small bubbles were clearly identifiable with a size from 1 to 2 mm. The formation of foam was instantaneously, it reached a height of 15 cm during a period of time of 20 seconds, then it decreased very fast. Ice formation was very thick, in some spots it was over 4 cm.

RUN No. 17

Spill of LNG on water

Composition: 84 % methane

16 % ethane

Mass spilled: 154.9 g

Volume spilled: 344 cm^3

Film: 4 - X Reversal 7277   200 ft   Focus 9   ASA 320

Camera speed: 200 F.P.S

Time elapsed: 40 s

Very explosive boiling with very turbulent turn over was noted. It was clearly observed the bimodel size distribution of the bubbles. The large bubbles had a size from 1 to 2 cm and they were located on the left side of the container during certain period of time; the small ones from 1 to 2 mm were on the right side. Foam formation took place immediately, it reached a height of 15 cm. After 10 seconds it reduced its level to 8 cm. Twenty seconds later, it was noticed that the bubbles size increased as the foam decreased. Both, bubbles and foam, disappeared few seconds later. LNG kept boiling very quietly. Ice formation took place immediately with no perforations.

RUN No. 18

Spill of LNG on water

Composition: 80 % methane

             11 % ethane

              9 % propane

Mass spilled: 140 g

Volume spilled: 311 cm^3

Film: Ektachrone 7242   200 ft   Focus 8   ASA 125

Camera speed: 100 F.P.S

Time elapsed: 80 s

Very violent boiling.   The bimodel size distribution of bubbles was for the large ones a size from 2 to 4 cm, and the small ones from 1 to 3 mm.   Foam formation took place immediately.   It reach a height of 2 cm and decreased very rapidly (after 10 seconds).   It was very clear observed how the LNG boiling rate decreased to a height of 2 cm and kept boiling. Ice formation was of a thickness from 1.5 to 2 cm.   After 15 seconds no perforations were on the ice layer.

RUN No. 19

Spill of LNG on water

Composition: 60 % methane

                        25 % ethane

                        15 % propane

Mass spilled: 189.6 g

Volume spilled: 420 cm^3

Film: Ektachrone 7242   200 ft   Focus 8   ASA 125

Camera speed: 200 F.P.S

Time elapsed: 40 s

Boiling was very violent. Foam reached 5 cm high. Boiling decreased but foam was present for 20 seconds with a bubble size from 1 to 2 mm. Ice formation was 2 cm thick with small perforations. After 20 seconds the foam started to decrease and it was observed how the LNG kept boiling very quietly during the remaining 20 seconds.

RUN No. 20

Spill of LNG on water

Composition: 5 % methane

　　　　　　　　95 % propane

Mass spilled: 383.2 g

Volume spilled: 800 cm^3

Film: Tri - X Reversal 7278 100 ft Focus 11 ASA 160

Camera speed: F.P.S

Time elapsed: 40 s

    Very quietly boiling was observed. The bimodel size distribution of bubbles was the big ones from 0.5 to 1 cm in diameter and the small ones from 1 to 2 mm. There was no foam formation. The ice layer was immediately formed with a tickness of 2.5 cm with no perforations. LNG kept boiling quietly with a height of 5 cm for a period of time of 10 minutes.

RUN No. 21

Spill of LNG on water

Composition: 99 % nitrogen

                  1 % propane

Mass spilled: 281.6 g

Volume spilled: 356.3 cm^3

Film: Tri - X Reversal 7278   100 ft   Focus 11   ASA 160

Camera speed: 100 F.P.S

Time elapsed: 40 s

As the spill was made, the boiling got violent and immediately very dense vapor clouds were formed. It was observed a high turbulence on the water surface with a slow rate of big bubbles (from 2 to 3 cm). In certain periods of time, it seemed that small bubbles (from 1 to 3 mm) were at the top of the boiling liquid. It was impossible to observe any foam formation because of the very dense clouds of vapor. There was no ice formation, just a very thin layer of ice around the walls of the container.

RUN No. 22

Spill of LNG on water

Composition: 95 % nitrogen

                5 % methane

Mass spilled: 274 g

Volume spilled: 351.78 cm^3

Film: Tri - X Reversal 7278   100 ft   Focus between 8 and 11

      ASA 160

Camera speed: 100 F.P.S

Time elapsed: 40 s

Moderate boiling occurred. A bimodel size distribution
of bubbles was very clearly defined with the formation of big
bubbles from 1 to 2 cm at the water surface, and small bubbles
from 1 to 2 mm above the big ones. Very consistent foam was
formed during a period of time of 30 seconds and with a height
of 10 cm. For the first time, the foam occurred over a liquid
boiling head of 4 cm which decreased slowly with time but the
foam remained consistent. There was no ice formation.

APPENDIX B

KINETIC MODEL FOR MIXTURES

In the theorethical consideration for mixtures, the state of the art for applying theory to both the thermodynamic and kinetic models of nucleation from a superheat, pure liquid, has been developed. The thermodynamic approach is essentially developed (Beegle, Modell, and Reid, 1974), but testing is required to predict the stability limits of superheated liquid mixtures. Several promising new equations of state applicable to liquids could be used (Reid, Prausnitz, and Sherwood, 1975). The implementation of the theory is not difficult but is time consuming and requires machine computation.

The more complex problem is to obtain a reasonable kinetic model for mixtures.

Several points must be considered. The first is the delineation of the correct surface tension. Presumably in the equilibrium situation, one could employ the value for the bulk mixture. However, for the dynamic growth-collapse phase, concentration gradients near the bubble surface may lead to a surface tension at the interface that is different from what might have been expected from the bulk liquid composition. This problem may be particularly important for mixtures in which there

is a larger difference in volatility between components.

Also, in mixtures, with a concentration gradient in the liquid phase, the more volatile component may be hindered from vaporization at the expected rates. Blander et al. (1971) consider this problem and solve the spherical diffusion equation $D(\partial C/\partial r)_{r=r_c}$ = rate of vaporization into a bubble for the case of one volatile component. They arrive at a correction factor to correct for the nucleation rate. Reiss (1950) and Hirschfelder (1974) have also suggested mathematical approaches to this problem.

Some of the difficulties in this analysis may be visualized better with the following case for a binary of A and B, both of which are volatile. To avoid the complexity of spherical geometry, consider a flat surface
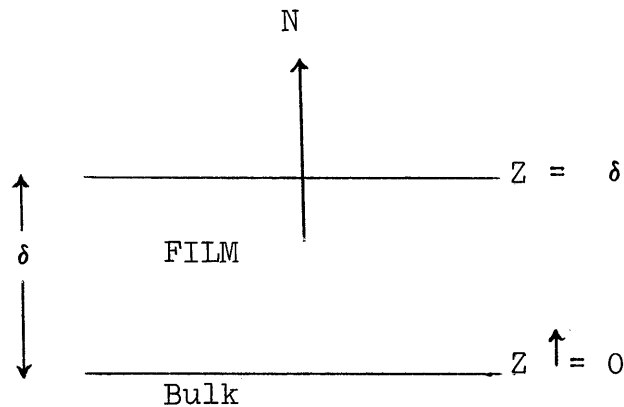
N represents the moles vaporizing from the surface/time. This vapor is in equilibrium with the surface at $Z = \delta$. As a

first approximation, neglect accumulation, and then the flux
of component A through the film is

$$N_A = -\rho^L D_A (\partial x_A / \partial Z) + x_A N = N y_A \qquad (1)$$

where x_A is a liquid mole fraction, y_A is the vapor mole frac-
tion, ρ^L is the film molal density, and D_A is the binary dif-
fusion coefficient. Rearranging Eq. (1),

with
$$-(\partial x_A / \partial Z) + \beta x_A = \beta y_A \qquad (2)$$
$$\beta = N / \rho^L D_A \qquad (3)$$

Then,
$$dx_A - \beta x_A dz = -\beta y_A dz \qquad (4)$$
$$x_A = C_1 e^{\beta Z} + y_A \qquad (5)$$

at $Z = 0$, $x_A = x_{A_B}$ = mole fraction in the bulk liquid, therefore

$$C_1 = x_{A_B} - y_A \qquad (6)$$

$$x_A = (x_{A_B} - y_A) e^{\beta Z} + y_A \qquad (7)$$

At the interface, x_{A_i} , $Z = \delta$ and

$$x_{A_i} = (x_{A_B} - y_A) e^{\beta \delta} + y_A \qquad (8)$$

Eq. (8) can be modified by noting

$$\beta \delta = \frac{N/\rho^L}{(D_A/\delta)} = \frac{N/\rho^L}{k} = \gamma_A \qquad (9)$$

k is the mass transfer coefficient.

$$\frac{x_{A_i} - y_A}{x_{A_B} - y_A} = e^{\gamma A} \tag{10}$$

If the mass transfer coefficient is large, $\gamma_A \sim 0$ and $e^\gamma \sim 1$. Then x_{A_i}, i.e., the mixture boils at the mixture bubble point in the film aroun the bubble.

However, if k is small, γ is large (as is e^γ) and $x_{A_B} \sim y_A$. The interpretation is then that the temperature on the bubbble film corresponds to the mixture dew point.

APPENDIX C

EXPANSION RATIO FOR BOILING MIXTURES

After a spill of LNG onto a warm surface, rapid vaporiza-
tion occurs. The gas which is formed rises as bubbles through
the liquid to the interface. Since a finite time is required
for the bubble to move from the boiling surface to the inter-
face, the "effective" liquid height is larger than the "non-
boiling" liquid height.

This expansion of the liquid due to rising vapor bubbles
is related to the rate of vapor evolution and the velocity of
rise.

Consider a mass of liquid boiling in a dike. Let the
liquid mass per unit area be m^L/A. If no boiling were pres-
ent, this would represent a liquid head of $m^L/A\rho^L$ where ρ^L
is the density of the liquid. Since boiling is taking place,
the true liquid-vapor interface is higher than $m^L/A\rho^L$. Let
the true height be h and define the expansion factor as where

$$\beta = \frac{h}{(m^L/A\rho^L)} \qquad (2)$$

To derive an expression for β ,

Area = A

(Non-boiling case)

true height = $h = \beta h_o$

Heat Flow to
Cause Boiling
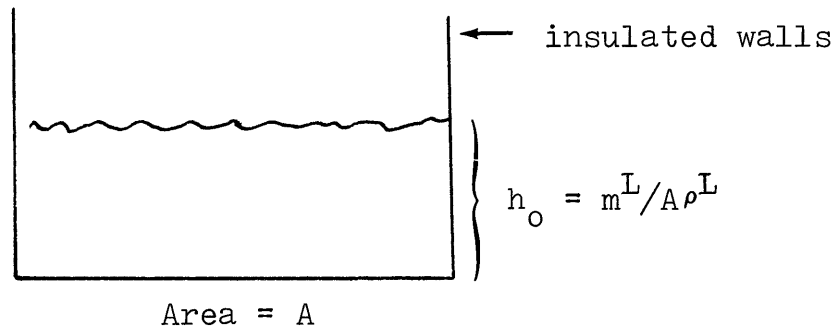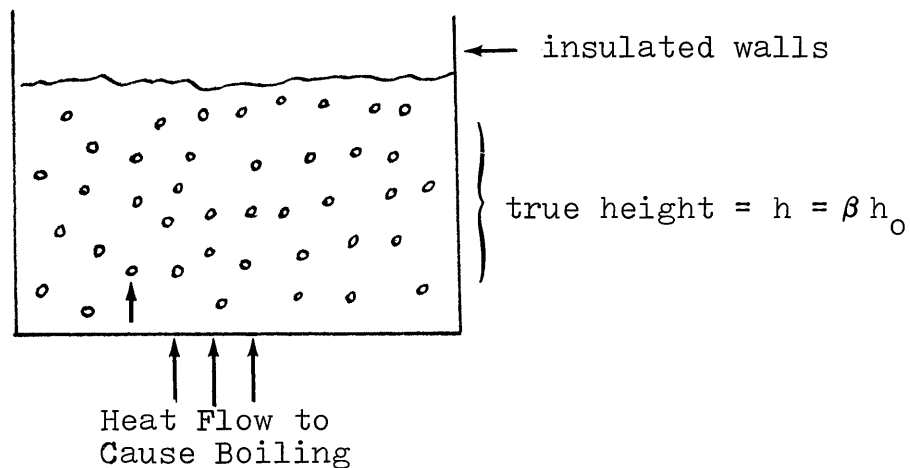
(Boiling case)

Let the volume of gas formed over area A per unit time be $\dot{G}$.
If the bubble rise velocity is u, then the time of rise of
any bubble is $\beta h_o/u = h/u$. The volume of gas in the liquid
is $\beta h_o \dot{G}/u$. Then, a volume balance gives

$$h_o A \quad + \quad \beta h_o \dot{G}/u \quad = \quad \beta h_o A \qquad (2)$$
$$\underbrace{}_{\text{liquid}} \qquad \underbrace{\phantom{\beta h_o \dot{G}/u}}_{\text{gas}} \qquad \underbrace{}_{\text{total}}$$

$$\beta = \frac{1}{1 - (\dot{G}/Au)} \qquad (3)$$

But $\dot{G}/A = (\dot{Q}/A)/\Delta H_v \rho^V = B/f(t)\Delta H_v \rho V \qquad (4)$

where ΔH is the heat of vaporization and ρ^V the density of the saturated vapor.

LITERATURE CITED

1. Arakawa, K., (1954) "Studies on the Freezing of Water: II Formation of Disc Crystals" J. Fac. Sci., Hokkaido Univ. Japan, Ser II, Vol. IV (5), 311.

2. Ibid, (1955) "Studies on the Freezing of Water: III Crystalography of Disc Crystal and Dendrites Developed from Disc Crystals" J. Fac. Sci., Hokkaido Univ. Japan, Ser II, Vol. IV (5), 355.

3. Beeagle, B.L., M. Modell, and R.C. Reid, (9174) AICHE J., 20: 1200.

4. Bigg, E.K., (1953) "The Supercooling of Water" Proc. Phys. Soc. B. 66, 688.

5. Blair, L.M. and J.A. Quinn, (1969) "The On-Set of Cellular Convection in a Fluid Layer with Time-Dependent Density Gradients" J. Fluid Mech. 36. (pt 2), 385.

6. Blander et. al (1971) Personal Communication with

Professor Robert C. Reid. November 29, 1972.

7. Bošnjakovic, F., (1930) "Verdampfung und Flussigkeits-
    uberhitzung" <u>Tech. Mech. Thermo-Dynam.</u> Berl. <u>1</u>, 358-
    62.

8. Carslaw, H.S. and J. C. Jaeger, (1959) <u>Conduction of
    Heat in Solids</u> 2nd ed. Oxford Univ. Press, London.

9. Chambre, P.L., (1956) "On the Dynamics of Phse Growth"
    Quart. J. Mech. and <u>Appl. Math.</u>, <u>IX</u>, pt 2, 244-233.

10. D.A. Booth, A. Bulsara, F.G. Joyce, I.P. Morton, and
    R.G. Scurlock, (1974) "Wall Film Flow Effects with
    Liquified Natural Gas" <u>Cryogenics</u> <u>9</u>, 561.

11. Deaton, W.M. and Frost, E.M., Jr., (1946) "Gas Hydrates
    and Their Relation to the Operation of Natural-Gas
    Pipelines" Mono <u>8</u>, <u>U.S. Department of Interior</u>, Bureau
    of Mines.

12. Dergarabedian, P., (1953) "The Rate of Growth of
    Vapor Bubbles in Superheated Water" <u>J. Appl. Mech.</u>

<u>20</u>, 537.

13.   Dergarabedian, P., (1960) "Observations on Bubble
      Growths in Various Superheated Liquids" <u>J. Fluid Mech</u>.
      pt 1, <u>9</u>, 39-48.

14.   E.M. Drake, A. Jeje, and R.C. Reid, (1975) "Trans-
      ient Boiling of Liquified Cryogens on a Water Surface"
      I. "Nitrogen, Methane, and Ethane", <u>Int. J. Heat Mass</u>
      <u>Transfer</u>., Vol. 18, 1361-1368.

15.   Forster, H.K. and N. Zuber, (1954) "Growth of a Vapor
      Bubble in Superheated Liquid" <u>J. Appl. Phys</u>. 25, 474-
      8.

16.   Gibson, D.C., (1972) "The Kinetic and Thermal Expan-
      sion of Vapor Bubbles" <u>J. Basic Engr</u>., March 89-96.

17.   Hammerschmidt, E.G., (1934) "Formation of Gas Hydrates
      in Natural Gas Transmission Lines" <u>Industrial and</u>
      <u>Engineering Chem</u>. <u>26</u>, (8), 851-5.

18. Hirschfelder, J.O., (1974) "Kinetics of Homogeneous
     Nucleation in Many Component Systems" Theoretical
     Chemistry Institute, University of Wisconsin, Madison,
     Wisconsin 53706.

19. Hovestrijdt, J., (1963) "The Influence of the Sur-
     face Tension Difference on the Boiling of Mixtures"
     Chem. Engr. Sci., 18, 631-9.

20. Jeje, A.,(1974) PH. D. Thesis, Chem. Eng. Dept.,
     M.I.T., Cambridge, Massachusetts.

21. Katz, D.L. et al, (1959) Handbook of Natural Gas
     Engineering. McGraw-Hill Co., Inc., N.Y.

22. Luborsky, F.E., (1959) "The Kinetics of Growth of
     Spherical Iron Crystallites in Mercury" J. Phys. Chem.
     61, 1336-1340.

23. Mason, B.J., (1958, a) "The Supercooling and Nuclea-
     tion of Water". Advances in Physics 7, 211.

24. Nukiyama, Shiro, (1934) "Maximum and Minimum Values
    of Heat Transmission from Metal to Boiling Water under
    Atmospheric Pressure", J. Soc. Mech. Engr. Japan, 37,
    367.

25. Plesset, M.S. and S.A. Zwick, (1952) "A Non-Steay
    Heat Diffusion Problem with Spherical Symmetry" J.
    Appl. Phys. 23 (1), 95-98

26. Plesset, M.S. and S.A. Zwick, (1954) "The Growth of
    Vapor Bubbles in Superheated Liquids" J. Appl. Phys.
    25 (4), 493-500.

27. Reid, R.C., Prausnitz, J.N., and Scherwood, T.K. (1975)
    "The Property of Gases and Liquids" McGraw-Hill Book
    Co. N.Y.

28. Reiss, H. (1950) "The Kinetics of Phase Transitions
    in Binary Systems" Chemical, Physics, J. Vol. 18,
    No. 6, 840-848.

29. Saito, S. Shazaburo, Marshall D.R. and Kobayashi, R.

"Hydrates at High Pressures: Pt II, Application of
Statistical Mechanics to the Study of Hydrates of
Methane, Argon, and Nitrogen" AICHE J. 10 (5), 743-
-40.

30.   Saito, S., Shazaburo and Kobayashi, R., (1965)
       "Hydrates at High Pressure: Pt III, Methane -
       Argon - Water, Argon - Nitrogen - Water Systems"
       AICHE J. 11 (1), 96-9.

31.   Saville, D.A., (1973) "The Effects of Interfacial
       Tension Gradients on the Motion of Drops and Bubbles"
       Chem. Engr. J., 5, 251-9.

32.   Schaefer, V.J., (1950) "The Formation of Frazil
       and Anchor Ice in Cold Water" Trans. Am. Geophys.
       Un. 31 (6), 885.

33.   Scriven, L.E., (1959) "On the Dynamics of Phase
       Growth" Chem. Engr. Sci. 10(1/2), 1-13.

34.   Scriven, L.E., (1960) "Dynamics of a Fluid Inter-
       face" Chem. Engr. Sci. 12, 98-108.

35. Scriven, L.E., (1962) "On the Dynamics of Phase Growth" Chem. Engr. Sci. 17, 55.

36. Skinner, L.A., (1963) Ph.D. Thesis, Northwestern Univ., Evanston, Illinois.

37. Thijssen H.A.C. (1955) Doct. Thesis, Agricultural University, Wageningen.

38. van Strahlen, S.J.D., (1966, 1967) "The Mechanism of Nucleate Boiling in Pure Liquids and in Binary Mixtures" Pt. I - IV. Int. J. Heat Mass Transfer, 9, 995-1046 (1966) 10, 1469-1498 (1967).

39. van Strahlen, S.J.D., (1968) "The Growth Rate of Vapor Bubbles in Superheated Pure Liquids and Binary Mixtures" Pt I and II. Int. J. Heat Mass Transfer, 11, 1467-1512

40. van Wijk, W.R., and Hovestreijdt, J., unpublished.

41. van Wijk, W.R., Vos, A.S., van Strahlen, S.J.D. (1956) Chem. Eng. Sci. Vol. 5, pp. 68-90.

42.   van Wijk, W.R., and van Strahlen, S.J.D. (1959)
       Dechema - Monogr. 32, 94.

43.   Wehmeyer, D.P. and T.W. Jackson, (1972) "Transient
       Film Boiling of Carbon Tetrachloride and Freon-113 on
       a Horizontal Cylindrical Surface" J. Heat Transfer,
       November.

44.   Wijk, W.R. van, Vos, A.S., van Strahlen, S.J.D.,
       (1956) "Heat Transfer to Boiling Binary Liquid Mix-
       tures" Che. Engr. Sc. 5, 68-80.

45.   Zuiderweg, F.J., and Harmes, A., (1958) Chem Eng. Sci.
       2, 89.